Solution of Hot Particle Ballooning Mode Integral Equation in Tokamaks

D. P. STOTLER* AND H. L. BERK

Institute for Fusion Studies, The University of Texas, Austin, Texas 78712

The solution for the stability of ballooning mode equations in tokamaks with hot particles is presented. The system of equations requires solving a combined set of differential and integral equations accounting for the detailed hot particle orbits. Special techniques are developed to describe the equilibrium, the linear set of matrix equations, and the boundary conditions. A modified WKB technique is developed to treat the boundary conditions. A detailed discussion is given of how boundary conditions are determined. We rigorously show why, in some cases, the eigenfunction may be exponentially growing with an outgoing group velocity. Sample results are presented. © 1987 Academic Press, Inc.

I. INTRODUCTION

A frequently proposed concept for improving plasma confinement is to use energetic particles. This idea has been studied in such varied devices as astron [1, 2], field-reversed ϑ-pinch [3], Elmo [4], bumpy Tori [5, 6], and mirror machines [7]. The currents produced by such particles form min-B wells that would produce MHD stability if the hot particles were completely decoupled from the background plasma [8–10]. However, it is important to ascertain how energetic the hot particles need to be in order for them to behave in a manner that is different from an MHD fluid, and whether or not there are additional modes of oscillation that can cause instability.

To answer some aspects of these questions for hot particles in tokamaks, we have developed a numerical method for solving the integral equation for ballooning modes in tokamaks in the high bounce frequency limit. The use of the ballooning mode representation was pioneered by Roberts and Taylor [11], who showed that with localized modes close to a single field line, there is a duality in considering the structure of an MHD-like mode. Traditionally, emphasizing the structure parallel to field line has been called the ballooning mode representation. Formal mathematical descriptions for treating the ballooning representations in toroidal geometry have been presented by Glasser [12], Lee and Van Dam [13], and Connor *et al.* [14].

---

* *Present address*: Princeton Plasma Physics Laboratory, Princeton University, Princeton, NJ 08540.

Integral equations for ballooning-like modes in tokamaks have been studied extensively for trapped particle instabilities [15, 16]. Only recently has the hot particle problem been of interest. Some numerical and analytic theories have been presented [17–22]. We have developed a code that can treat arbitrary hot particle distribution functions; our inversion technique does not depend on knowing beforehand the form of the perturbed eigenfunctions.

In solving the integro-differential set of equations, several conceptual physical and numerical issues must solved. They are as follows: (1) An equilibrium model is needed; it is found by using a method developed by Rosenbluth *et al.* [10] that considers a circular flux surface under the assumption of large aspect ratio. (2) Boundary conditions are required for the linearized equations. We show that out-going wave boundary conditions should be invoked. We introduce a modified WKB method in order to apply the boundary conditions accurately and efficiently. The outgoing waves give a dissipative mechanism that is crucial to the stability properties of the problem. The WKB method allows accurate numerical solutions to be obtained by integrating only over a few (2–3) poloidal periods. (3) The question of mode localization is a crucial aspect of this study. For many equilibrium parameters we find that modes do not localize spatially. In such cases we show that stability requires an investigation of the continuous spectrum which is the wave spectrum found by studying the operator in the limit that the distance along a field line becomes large. In the Appendix we generalize the method used for describing convective and absolute instabilities to show that if the continuous spectrum can be stablized, the global eigenmodes will be spatially localized.

The primary purpose of this paper is to present the numerical techniques and the theory needed to obtain correct numerical solutions. A more complete study of the physical issues will be presented elsewhere [20, 21].

II. Basic Equations

The equations that we wil use to describe electromagnetic perturbations arising in tokamak and mirror systems containing energetic particles have been derived by several authors [23, 24]. We expect mode frequencies to be on the order of the energetic particle magnetic drift frequency. Thus, we can assume that the energetic particle bounce frequency ω_b is large relative to the mode frequency and the magnetic drift frequency if $\omega_b > \omega_d$. Their ratio can be written approximately as

$$\frac{\omega_b}{\omega_d} \sim \frac{1}{l} \frac{v_\parallel}{v_\perp} \frac{r}{a_L} \frac{R}{L},$$

where l is the toroidal mode number, $v_\parallel/v_\perp$ is the ratio of the parallel to perpendicular velocities for the trapped species, a_L is a typical Larmor radius, r is the radial scale length for the device, and R is the radius of curvature of its magnetic

mirror field (the major radius). L representes the typical length of a bounce orbit. Because of the appearance of r/a_L here, the large bounce frequency approximation is excellent for electrons, and quite accurate for ions if $l \lesssim 10$.

We will take as our starting point the high-mode-number (i.e., short perpendicular wavelength) limit of the expression for the quadratic form obtained by Antonsen and Lee [23]. In this limit the most unstable modes vary rapidly across the field lines and slowly along them. They arrived at this result from the linearized guiding center equations of motion derived from the bounce-averaged drift-kinetic equation. For simplicity, we do not consider here the equilibrium electrostatic potential effect included in their treatment.

The magnetic field displacement vector is written in the form $\xi = \hat{\xi}(x) \exp[iS(\mathbf{x})]$, where S is the eikonal with $\hat{b} \cdot \nabla S = 0$; it provides the short-wavelength behavior perpendicular to the magnetic field. $\hat{\xi}$ is a slowly varying amplitude; it can be decomposed into two components: $\hat{\xi} = X\hat{b} \times \nabla S + Y\nabla S$. To prevent the compressional term from dominating, we must have $Y \ll X$. Then

$$\frac{1}{2} \int d^3x \left[\sigma \, |\nabla S|^2 \, |\hat{b} \cdot \nabla(XB)|^2 + \tau \, |\hat{Q}_L|^2 - |XB|^2 \, \hat{e} \cdot \kappa \left(\frac{\sigma}{\tau} \hat{e} \cdot \hat{\nabla} P_\perp + \hat{e} \cdot \hat{\nabla} P_\parallel \right) \right.$$

$$- \frac{\rho \omega(\omega - \omega_{*i})}{B^2} |XB|^2 \, |\nabla S|^2 - \sum_{e,i} m \int d^3v$$

$$\left. \times \left\{ \left| \left\langle v_\parallel^2 \hat{e} \cdot \kappa(XB) + \mu \left[\hat{Q}_L + B\frac{\sigma}{\tau} \hat{e} \cdot \kappa(XB)) \right] \right\rangle \right|^2 \times \frac{\omega - \omega_*}{\omega - \langle \omega_d \rangle} \frac{\partial F}{\partial E} \right\} \right] = 0, \quad (1)$$

where

$$\sigma = 1 + \frac{P_\perp - P_\parallel}{B^2}, \qquad \tau = 1 + \frac{1}{B} \frac{\partial P_\perp}{\partial B}, \qquad \hat{e} = \frac{\hat{b} \times \nabla S}{B}, \qquad \kappa = \hat{b} \cdot \nabla \hat{b},$$

$$\hat{b} = \mathbf{B}/B, \qquad \hat{Q}_L = Q_L - \frac{\sigma}{\tau} B\hat{\xi} \cdot \kappa, \qquad Q_L = B_\parallel + \hat{\xi} \cdot \nabla B,$$

$$B_\parallel = \hat{b} \cdot \nabla \times (\hat{\xi} \times \mathbf{B}), \qquad \hat{\nabla} = \nabla - \nabla B \frac{\partial}{\partial B}, \qquad \rho = m_i n_i, \qquad \omega^* = \frac{B}{\Omega} \frac{\hat{e} \cdot \nabla F}{\partial F/\partial E},$$

$$\omega_d = -\frac{B}{\Omega} (v_\parallel^2 \hat{e} \cdot \kappa + \mu \hat{e} \cdot \nabla B), \qquad \mu = \frac{v_\perp^2}{2B}, \qquad E = \mu B + v_\parallel^2,$$

$$\langle \cdots \rangle \equiv \frac{\int dl(\cdots)/|v_\parallel|}{\int dl/|v_\parallel|}.$$

$\Omega = qB/m = $ cyclotron frequency, and m and q are the particle mass and charge, respectively.

To get a form appropriate for a three-component plasma such as in EBT, the

kinetic term for the core electrons and ions is replaced by the conventional form in which $\omega \sim \omega_{*i} \gg \omega_d$. The term

$$\omega_{*i} = \frac{-B}{m_i n_i} \sum_j \frac{\hat{e} \cdot \nabla P_{\perp j}}{\Omega_j}$$

representing the ion diamagnetic drift has been included in the quadratic form. For example, this term follows from the work of Catto, Hastie, and Connor [24] if $\beta \equiv 2(P_\perp + P_\parallel)/B^2$ is sufficiently small. The subscript i refers to ions.

We now set $\phi = XB$ in Eq. (1) and vary with respect to ϕ^* and Q_L^* so that

$$\mathbf{B} \cdot \nabla \left[\frac{\sigma |\nabla S|^2 (\mathbf{B} \cdot \nabla \varphi)}{B^2} \right] + \sigma B \hat{e} \cdot \boldsymbol{\kappa} \left(Q_L - \frac{\sigma}{\tau} \varphi B \hat{e} \cdot \boldsymbol{\kappa} \right)$$

$$+ \varphi \hat{e} \cdot \boldsymbol{\kappa} \left(\frac{\sigma}{\tau} \hat{e} \cdot \hat{\nabla} P_\perp + \hat{e} \cdot \hat{\nabla} P_\parallel \right) + \omega(\omega - \omega_{*i}) \frac{|\nabla S|^2}{V_A^2} \varphi$$

$$= m_h \int d^3 v \frac{\omega - \omega_*}{\omega - \langle \omega_d \rangle} \frac{\partial F_h}{\partial E} v_\parallel^2 \hat{e} \cdot \boldsymbol{\kappa} (\langle v_\parallel^2 \hat{e} \cdot \boldsymbol{\kappa} \varphi + \mu Q_L \rangle), \qquad (2)$$

and

$$\tau \left(Q_L - \frac{\sigma}{\tau} \varphi B \hat{e} \cdot \boldsymbol{\kappa} \right) = m_h \int d^3 v \frac{\omega - \omega_*}{\omega - \langle \omega_d \rangle} \frac{\partial F_h}{\partial E} \mu (\langle v_\parallel^2 \hat{e} \cdot \boldsymbol{\kappa} \varphi + \mu Q_L \rangle), \qquad (3)$$

where φ represents the perturbed electrostatic potential and Q_L is the parallel (to the equilibrium field) perturbed magnetic field in the Lagrangian frame. $V_A^2 = B^2/\rho$ is the square of the Alfvén velocity. The subscript h refers to the energetic species.

Since the energetic particles are trapped in a rather shallow magnetic well, their parallel pressures and velocities are much smaller than the perpendicular values. In particular, it can be shown that $v_\parallel^2 \sim (r/R) v_\perp^2$ (r and R are the minor and major radii of the torus, respectively). These quantities then enter into the equation a factor of order $\sim r/R$ smaller than the dominant terms. Thus, we can reasonably neglect the parallel velocity and pressure effects for the trapped particles, resulting in a significantly simplified set of equations,

$$\mathbf{B} \cdot \nabla \left[\frac{\sigma |\nabla S|^2}{B^2} (\mathbf{B} \cdot \nabla \varphi) \right] + \sigma B_{\bar{e}} \cdot \boldsymbol{\kappa} \left(Q_L - \frac{\sigma}{\tau} \varphi B \hat{e} \cdot \boldsymbol{\kappa} \right)$$

$$+ \varphi \hat{e} \cdot \boldsymbol{\kappa} \left(\frac{\sigma}{\tau} \hat{e} \cdot \hat{\nabla} P_\perp + \hat{e} \hat{\nabla} P_{\parallel,c} \right) + \omega(\omega - \omega_{*i}) \frac{|\nabla S|^2}{V_A^2} \varphi = 0, \qquad (4)$$

$$\tau \left(Q_L - \frac{\sigma}{\tau} \varphi B \hat{e} \cdot \boldsymbol{\kappa} \right) = m_h \int d^3 v \frac{\omega - \omega_*}{\omega - \langle \omega_d \rangle} \frac{\partial F_h}{\partial E} \mu^2 \langle Q_L \rangle. \qquad (5)$$

Because of the remaining integral term in Eq. (5), these equations are still very difficult to solve analytically. However, some progress can be made if the trapped particles are assumed to be deeply trapped [10, 19]; that is, the bounce averages cover only a short distance along the field line, and we can assume for some variable α: $\langle \alpha \rangle \simeq \alpha(s = s_0)$, where s_0 is the center point of the bounce trajectory. Also, evaluating the velocity integral can be facilitated if it is appropriate to assume $\omega \ll \langle \omega_d \rangle$. This procedure was implemented by Rosenbluth *et al.* [10] and by Connor *et al.* [17] to obtain a simplfied numerical model. Their results indicated that the energetic particles could indeed stabilize the MHD-like ballooning modes (if one assumes $\omega \ll \langle \omega_d \rangle$) and allow access to the second-stability region [25]. Since we seek to treat modes having $\omega \lesssim \langle \omega_d \rangle$ (the precessional drift-resonant instability) as well as the more familiar case in which $\omega \ll \langle \omega_d \rangle$, their low frequency assumption is not valid. We would also like to be able to consider distribution functions containing large percentages of nearly marginally trapped particles (sloshing ion distributions); thus, the deeply trapped approximation is not applicable either. As a result, we must numerically solve Eqs. (4) and (5) as they are written above.

Some simplicity is achieved by considering a large aspect ratio equilibrium in which the flux surfaces are shifted circles [10]. If the plasma beta is small with a sharp gradient, reasonable results can be obtained analytically for the various equilibrium quantities needed. We write the magnetic field in the Clebsch form, $\mathbf{B} = \nabla \psi \times \nabla \beta$. ψ is the solution of the anisotropic equilibrium equation derived by Grad [26],

$$R^2 \nabla \cdot (R^{-2} \nabla \psi) + \nabla \psi \cdot \nabla \ln \sigma = -\frac{1}{\sigma^2} \frac{\partial G(\psi)}{\partial \psi} - \frac{R^2}{\sigma} \frac{\partial P_\parallel(\psi)}{\partial \psi}, \tag{6}$$

where R is the cylindrical coordinate representing the major radius of the torus, $G = (\sigma R B_T)^2/2$ (B_T is the toroidal component of the magnetic field; note that G is a function of ψ only), and $\sigma = 1 + (P_\perp - P_\parallel)/B^2$. We will use a flux coordinate system (ψ, ϑ, ζ) to describe the equilibrium. The eikonal S is usually written in the form

$$S = n(q\vartheta - \zeta), \tag{7}$$

with

$$\mathbf{B} = \nabla \psi \times \nabla \beta = \nabla \psi \times \nabla(q\vartheta - \zeta);$$

we assume $\nabla S = n \nabla \beta$, although S is in general also a function of ψ. To determine and expression for $\mathbf{k}_\perp = \nabla S$, we need to calculate $\nabla \vartheta$ so that we can use Eq. (7). Equivalently, we can calculate $\nabla \beta$. Clearly,

$$\nabla \beta = \frac{\mathbf{B} \cdot \nabla \psi}{|\nabla \psi|^2} + \lambda \nabla \psi. \tag{8}$$

and it can be shown [10] that λ is given by

$$\mathbf{B}_p \cdot \nabla \lambda = \nabla \cdot \left(\frac{B_T}{R} \frac{\nabla \psi}{|\nabla \psi|^2} \right), \tag{9}$$

where B_p is the poloidal component of the magnetic field.

To solve the equilibrium equation, we will assume large aspect ratio $(r/R \ll 1)$, low-β $(\beta \ll 1)$, and localized gradients $[\Lambda \equiv (\nabla \ln P)^{-1} \ll r]$, so that the flux surfaces are, to first order in $\varepsilon = r/R$, shifted circles [10]. We use a coordinate system in which $R = R_0 + r \cos \vartheta$ and expand ψ in powers of ε:

$$\psi(r, \vartheta) = \psi_0(r) + \psi_1(r, \vartheta) + \cdots. \tag{10}$$

In this coordinate system, $B_T \simeq B_{T0}(1 - \varepsilon \cos \vartheta)$, $B_p = B_{p0}(r) + O(\varepsilon)$, $B_{p0} = (d\psi_0/dr)/R_0$, $B_p/B_T \sim O(\varepsilon)$, and the safety factor $q = r B_{T0}/R_0 B_{p0} + O(\varepsilon)$. First, we note that the term $\nabla \psi \cdot \nabla \ln \sigma$ in Eq. (6) is $\sim \varepsilon^2$ smaller than $(R^2/\sigma) \, \partial P_\parallel/\partial \psi$, so that it may be dropped. Except in $G(\psi)$, we can set $\sigma = 1$ due to the low-β and short gradient scale length approximations. Using these results, we can now write

$$R^2 \nabla \cdot R^{-2} \nabla \psi = -\frac{\partial}{\partial \psi} (G + R_0^2 P_c) - 2r R_0 \cos \vartheta \frac{\partial P_c}{\partial \psi}$$

$$- R_0^2 \left(1 + 2 \frac{r}{R_0} \cos \vartheta \right) \frac{\partial P_{\parallel h}}{\partial \psi} + O(\varepsilon^2). \tag{11}$$

The subscript c refers to the isotropic core plasma and h to the energetic trapped component. We add and subtract

$$\overline{\frac{\partial P_{\parallel h}}{\partial \psi}} \equiv \frac{1}{2\pi} \int_0^{2\pi} d\vartheta \frac{\partial P_{\parallel h}}{\partial \psi}$$

in Eq. (11); it will be seen later that this allows $\psi_1(r, \vartheta)$ to be periodic in ϑ. Thus,

$$R^2 \nabla \cdot (R^{-2} \nabla \psi) = -\frac{\partial}{\partial \psi} (G + R_0^2 P_c) - R_0^2 \overline{\frac{\partial P_{\parallel h}}{\partial \psi}}$$

$$- 2r R_0 \cos \vartheta \frac{\partial P_c}{\partial \psi} - R_0^2 \left(\frac{\partial P_{\parallel h}}{\partial \psi} - \overline{\frac{\partial P_{\parallel h}}{\partial \psi}} \right) + O(\varepsilon^2), \tag{12}$$

where we have assumed that $\partial P_{\parallel h}/\partial \psi \sim \varepsilon \partial P_c/\partial \psi$; this follows from the trapped particle nature of the hot species with the understanding that $P_{\perp h} \sim P_c$.

We define the lowest-order part of the right-hand side of Eq. (12):

$$J(\psi) \equiv \frac{\partial}{\partial \psi}(G + R_0^2 P_c) + R_0^2 \overline{\frac{\partial P_{\parallel h}}{\partial \psi}}.$$

Then,

$$R^2 \nabla \cdot (R^{-2} \nabla \psi_0) = -J(\psi_0), \tag{13}$$

and

$$R^2 \nabla \cdot (R^{-2} \nabla \psi_1) = -2rR_0 \cos \vartheta \frac{\partial P_c(\psi_0)}{\partial \psi} - R_0^2 \left(\frac{\partial P_{\parallel h}}{\partial \psi} - \overline{\frac{\partial P_{\parallel h}}{\partial \psi}} \right) - \psi_1 \frac{\partial J(\psi_0)}{\partial \psi}. \tag{14}$$

It can be shown that the last term in Eq. (14) is smaller than the others by a factor of Δ/r, and can be neglected in our approximation. Using similar orderings, we find that

$$\nabla \cdot \left(\frac{B_T \nabla \psi}{R |\nabla \psi|^2} \right) = \frac{1}{rR_0} \frac{\partial q}{\partial r} - \frac{B_{T0}}{R_0^3 B_{p0}} \frac{1}{r} \frac{\partial}{\partial r} \left(r \frac{\partial \psi_1}{\partial r} \right) + O\left(\varepsilon \frac{\Delta}{r} \right). \tag{15}$$

Then, from Eqs. (9), (14), and (15),

$$\lambda = \frac{1}{B_{p0} R_0} \frac{\partial q}{\partial r} (\vartheta - \vartheta_k) + \frac{2B_{T0} r^2}{R_0^2 B_{p0}^3} \frac{\partial P_c}{\partial \psi} (\sin \vartheta - \sin \vartheta_k)$$

$$+ \frac{B_{T0} r}{R_0 B_{p0}^3} \int^{\vartheta} d\vartheta' \frac{\partial}{\partial \psi} (P_{\parallel h} - \overline{P_{\parallel h}}); \tag{16}$$

here, ϑ_k is introduced as the origin of the integrations and represents the radial wavenumber. In tokamak geometry, the variable along the field line, ϑ, is extended to cover the range $-\infty < \vartheta < +\infty$. It will be convenient to write the trapped particle pressure functions in the form

$$P_{\parallel h}(\vartheta) = 2\hat{P}_{\perp h} \rho(\psi)(r/R_0) p_{\parallel}(\vartheta) \tag{17}$$

and

$$P_{\perp h}(\vartheta) = \hat{P}_{\perp h} \rho(\psi) p_{\perp}(\vartheta), \tag{18}$$

with $p_{\perp}(\vartheta = 0) = 1$, $p_{\parallel,\perp}(|\vartheta \bmod 2\pi| > \vartheta_0) \equiv 0$, and $\rho(\psi)$ containing all of the radial dependence. It follows that

$$\lambda \nabla \psi = \frac{q}{r} \{ S(\vartheta - \vartheta_k) - \alpha_c(\sin \vartheta - \sin \vartheta_k) - \alpha_h [g(\vartheta) - g(\vartheta_k)] \} \hat{r} + O(\varepsilon), \tag{19}$$

where

$$S = \frac{r}{q} \frac{\partial q}{\partial r},$$

$$\alpha_c \equiv -\frac{2r^2}{B_{p0}} \frac{\partial P_c}{\partial \psi},$$

$$\alpha_h \equiv -\frac{2r^2}{B_{p0}} \hat{P}_{\perp h} \frac{\partial \rho}{\partial \psi},$$

$$g(\vartheta) = p(\tilde{\vartheta}) - \frac{\tilde{\vartheta}}{\pi} p(\vartheta_0), \qquad\qquad 0 < \tilde{\vartheta} < \vartheta_0$$

$$= \left(1 - \frac{\tilde{\vartheta}}{\pi}\right) p(\vartheta_0), \qquad\qquad \vartheta_0 < \tilde{\vartheta} < 2\pi - \vartheta_0, \quad \tilde{\vartheta} = \vartheta \bmod 2\pi$$

$$= \left(\frac{2\pi - \tilde{\vartheta}}{\pi}\right) p(\vartheta_0) - p(2\pi - \tilde{\vartheta}), \qquad 2\pi - \vartheta_0 < \tilde{\vartheta} < 2\pi,$$

and

$$p(\vartheta) = \int_0^\vartheta d\vartheta' \, p_\parallel(\vartheta').$$

Finally,

$$\nabla \beta = \frac{q}{r} [\hat{\vartheta} + h(\vartheta) \, \hat{r}], \qquad\qquad (20)$$

with $h(\vartheta) = S(\vartheta - \vartheta_k) - \alpha_c(\sin \vartheta - \sin \vartheta_k) - \alpha_h[g(\vartheta) - g(\vartheta_k)]$.

The next section of this chapter will examine trapped particle distributions that are peaked near $\vartheta = 0$. We will model this with the distribution function

$$F_h[\mu, E, \psi(r)] = \alpha_F \left[1 - \frac{(r - r_0)^2}{\Delta r^2}\right] (\mu B_c - E) \, e^{-E/T}, \qquad \frac{E}{B_c} < \mu < \frac{E}{B_{min}}$$

$$= 0, \qquad\qquad\qquad\qquad 0 < \mu < \frac{E}{B_c}, \qquad (21)$$

where

$$\alpha_F = \frac{4\hat{P}_{\perp b}}{m_h \sqrt{2\pi} \, T^{7/2}} \frac{1}{(1 - B_{min}/B_c)^{3/2}(1 + 4B_c/B_{min})},$$

$B_{min} = B \, (\vartheta = 0)$, $B_c = B \, (\vartheta = \vartheta_0)$, and ϑ_0 represents the maximum extent of the hot particles in $\vartheta \bmod 2\pi$. It can then be shown that

$$p_\perp(\vartheta) = \frac{(1 - B/B_c)^{3/2}(1 + 4B_c/B)}{(1 - B_{min}/B_c)^{3/2}(1 + 4B_c/B_{min})},$$

and

$$p_{\parallel}(\vartheta) = \frac{R_0}{r} \frac{B_c}{B} \frac{(1 - B/B_c)^{5/2}}{(1 - B_{min}/B_c)^{3/2}(1 + 4B_c/B_{min})}.$$

Note that to within factors of order ε, $p_{\perp}(\vartheta) \simeq (\cos\vartheta - \cos\vartheta_0)^{3/2}/(1 - \cos\vartheta_0)^{3/2}$.

We will also consider two "sloshing" distributions in which $p_{\perp}(\vartheta)$ peaks near ϑ_0. The first one again contains only trapped particles and is given by

$$F_h[\mu, E, \psi(r)] = \alpha_F \left[1 - \frac{(r - r_0)^2}{\Delta_r^2} \right] \frac{(\mu B_c - E) e^{-E/T}}{[1 + (\mu B_c/E - 1)^2/\Delta\lambda^2]}, \qquad \frac{E}{B_c} < \mu < \frac{E}{B_{min}}$$

$$= 0, \qquad\qquad\qquad\qquad\qquad\qquad\qquad\qquad\qquad 0 < \mu < \frac{E}{B_c}, \qquad (22)$$

where

$$\alpha_F = \frac{16 B_c^{3/2} P_{\perp h}}{15 \sqrt{\pi} \, m_h \, T^{7/2} C(0)},$$

$$C(\vartheta) \equiv B^{3/2} \int_1^{B_c/B} \frac{d\lambda\lambda}{\sqrt{B_c/B - \lambda}} \frac{(\lambda - 1)}{[1 + (\lambda - 1)^2/\Delta\lambda^2]},$$

so that $p_{\perp}(\vartheta) = C(\vartheta)/C(0)$. Now, $p_{\perp}(\vartheta)$ and $p_{\parallel}(\vartheta)$ cannot be calculated analytically. Instead, they are computed numerically on a grid at the beginning of the program, and values at arbitrary ϑ are obtained by interpolation.

We also consider a distribution containing circulating as well as trapped energetic particles:

$$F_h[E, \mu, \psi(r)] = \alpha_F \left[1 - \frac{(r - r_0)^2}{\Delta_r^2} \right] \frac{E e^{-E/T}}{[1 + (\mu B_c/E - 1)^2/\Delta\lambda^2]}, \qquad (23)$$

where in this case

$$C(\vartheta) = B^{3/2} \int_0^{B_c/B} \frac{d\lambda\lambda}{\sqrt{B_c/B - \lambda}} \frac{1}{[1 + (\lambda - 1)^2/\Delta\lambda^2]},$$

and $\vartheta_0 \equiv \pi$. The normalization factor α_F is the same as for Eq. (22). In the limit of high transit frequency (analogous to the bounce frequency for trapped particles), the passing particles do not contribute to the kinetic term [27]. Thus, the magnetic moment integral in Eq. (3) ranges from E/B_c to E/B in all cases so that only trapped particles are included.

The parameter $\Delta\lambda$ in Eqs. (22) and (23) allows the shape of the perpendicular pressure profile to be varied continuously from one peaking at $\vartheta = 0$ ($\Delta\lambda \gg 1$) to one peaking near $\vartheta = \vartheta_0$ ($\Delta\lambda \ll 1$). These sloshing distributions are introduced in an attempt to stabilize the high frequency ($\omega \lesssim \langle \omega_d \rangle$) precessional mode. The physical

motivation for this choice and the detailed results of the investigation will be reported elsewhere [21, 22].

Before inserting the equilibrium functions into Eqs. (4) and (5), we note that numerical solution of the equations will be simplified if we change to new variables,

$$\delta Q \equiv Q_{\mathrm{L}} - \frac{\sigma}{\tau} \varphi B \hat{e} \cdot \mathbf{\kappa},$$

$$\phi \equiv (1 + h^2)^{1/2} \varphi;$$

note that $\delta Q = 0$ in regions where there are no energetic particles. Thus, Eqs. (4) and (5) become

$$D_{\mathrm{op}} \phi \equiv \sigma \frac{d^2 \phi}{d\vartheta^2} - \frac{\sigma \phi}{1 + h^2} \left[\frac{(dh/d\vartheta)^2}{(1 + h^2)} + h \frac{d^2 h}{d\vartheta^2} \right] + \left(\frac{d\phi}{d\vartheta} - \frac{h(dh/d\vartheta)\,\phi}{1 + h^2} \right) \frac{d\sigma}{d\vartheta}$$

$$+ \frac{\phi D(\vartheta)}{(1 + h^2)} \left\{ \frac{\alpha_{\mathrm{c}}}{2} \left(1 + \frac{\sigma}{\tau} \right) + \frac{\alpha_{\mathrm{h}}}{2} \frac{\sigma}{\tau} p_{\perp}(\vartheta) \right\} + \frac{q^2 R_0^2}{V_{\mathrm{A}}^2} \omega(\omega - \omega_{*i}) \phi$$

$$= -\frac{q r R_0 \sigma D(\vartheta)}{(1 + h^2)^{1/2}} \delta Q, \tag{24}$$

and

$$\tau \delta Q = m_{\mathrm{h}} \int d^3 v \, \frac{\omega - \omega_*}{\omega - \langle \omega_{\mathrm{d}} \rangle} \mu^2 \frac{\partial F_{\mathrm{h}}}{\partial E} \left[\langle \delta Q \rangle + \frac{q}{r R_0} \left\langle \frac{\sigma}{\tau} \frac{D(\vartheta)\,\varphi}{(1 + h^2)^{1/2}} \right\rangle \right], \tag{25}$$

where $D(\vartheta) = \cos \vartheta + h(\vartheta) \sin \vartheta$. We write ω_{*i} as

$$\omega_{*i} = -\omega_{*0} \left(\alpha_{\mathrm{c}} + 2 \frac{Z_i}{Z_{\mathrm{h}}} \frac{m_{\mathrm{h}}}{m_i} \left\{ \frac{(1 - \tau)}{\tau} \left[\alpha_{\mathrm{c}} - 2\sigma q^2 D(\vartheta) \right] + \frac{\alpha_{\mathrm{h}} p_{\perp}(\vartheta)}{\tau} \right\} \right)$$

$$\frac{\omega_{*0}}{\omega_{\mathrm{A}}} = \frac{n V_{\mathrm{A}}}{4 r \Omega_i}, \qquad \omega_{\mathrm{A}} = \frac{V_{\mathrm{A}}}{q R_0},$$

with Z_j the atomic number of species j.

To solve Eqs. (24) and (25), we expand δQ and ϕ,

$$\delta Q \equiv \sum_{l=1}^{\infty} q_l f_l(\vartheta), \tag{26}$$

$$\phi \equiv \phi_{\mathrm{h}}(\vartheta) + \sum_{l=1}^{\infty} q_l \phi_l(\vartheta), \tag{27}$$

with

$$f_l(\vartheta) \equiv \cos \left[(2l - 1) \frac{\pi \bar{\vartheta}}{2 \vartheta_0} \right], \qquad |\bar{\vartheta}| < \vartheta_0$$

$$\equiv 0, \qquad |\bar{\vartheta}| > \vartheta_0 \qquad \bar{\vartheta} = \vartheta \bmod 2\pi;$$

ϕ_h and the ϕ_l's are found by itegrating

$$D_{op}\phi_h = 0, \tag{28}$$

$$D_{op}\phi_l = \frac{qrR_0 D(\vartheta)\,f_l(\theta)}{(1+h^2)^{1/2}} \tag{29}$$

over each 2π region in the range of ϑ, $0 < \vartheta < \infty$. Equation (28) is integrated with $\phi_h = \phi$ and $d\phi_h/d\vartheta = d\phi/d\vartheta$ at the beginning of an integration over one period. The same is done with Eq. (29), but $\phi_l = 0$ and $d\phi_l/d\vartheta = 0$ are employed as initial values.

Once the functional forms of ϕ_h and ϕ_l are known, they can be used to calculate the matrix elements of a set of linear equations for the q_l's obtained from Eq. (25). Namely,

$$\sum_{l=1}^{N} q_l A_{ll'} = B_{l'}, \tag{30}$$

$$A_{ll'} = \int_0^{\vartheta_0} d\vartheta\, \tau B_c f_l f_{l'}/B + \frac{\alpha_h}{5(1-\cos\vartheta)^{3/2}\, q^2\varepsilon^2} \int_1^{\lambda_m} d\lambda\lambda^{3/2}$$

$$\times \left\{ \frac{\Delta_r}{R}\left[1 - \frac{(r-r_0)^2}{\Delta_r^2}\right] \frac{\omega}{\omega_{d0}} I_{5/2} \right.$$

$$+ (\lambda-1)\left(\frac{\omega}{\omega_{d0}}\frac{\Delta_r}{R}\left[1-\frac{(r-r_0)^2}{\Delta_r^2}\right]+1\right) I_{7/2}\right\} \tilde{f}_{l'}\left\{\tilde{f}_l + \overline{\left[\frac{\phi_l\sigma q^2 D(\vartheta)}{\tau(1+h^2)^{1/2}}\right]}\right\}, \tag{31}$$

$$B_{l'} = -\frac{\alpha_h}{5(1-\cos\vartheta)^{3/2}\, q^2\varepsilon^2}\int_1^{\lambda_m} d\lambda\lambda^{3/2}\left\{\frac{\Delta_r}{R}\left[1-\frac{(r-r_0)^2}{\Delta_r^2}\right]\frac{\omega}{\omega_{d0}} I_{5/2}\right.$$

$$+ (\lambda-1)\left(\frac{\omega}{\omega_{d0}}\frac{\Delta_r}{R}\left[1-\frac{(r-r_0)^2}{\Delta_r^2}\right]+1\right) I_{7/2}\right\} \tilde{f}_{l'}\overline{\left[\frac{\phi_h\sigma q^2 D(\vartheta)}{\tau(1+h^2)^{1/2}}\right]}, \tag{32}$$

where we have defined

$$\lambda_m = \frac{1-\varepsilon\cos\vartheta}{1-\varepsilon}, \qquad \lambda = \frac{\mu B_c}{E} = \frac{1-\varepsilon\cos\vartheta_0}{1-\varepsilon\cos[\vartheta_T(\lambda)]}, \qquad \omega_{d0} = \frac{nqT}{rR\Omega_h},$$

$\Omega_h =$ hot particle cyclotron frequency,

$$\bar{\alpha} \equiv \frac{1}{2}\int_{-\vartheta_T(\lambda)}^{\vartheta_T(\lambda)} d\vartheta\, \frac{\alpha(\vartheta)}{\sqrt{\cos\vartheta-\cos\vartheta_T}},$$

$$I_{5/2} = \frac{1}{\sqrt{\pi}}\int_0^\infty \frac{dz z^{5/2} e^{-z}}{(\omega/\omega_{d0})\,I_1 + \lambda z f(\lambda)},$$

$$I_{7/2} = \frac{1}{\sqrt{\pi}}\int_0^\infty \frac{dz z^{7/2} e^{-z}}{(\omega/\omega_{d0})\,I_1 + \lambda z f(\lambda)}.$$

We also calculate

$$\frac{1}{\sqrt{\pi}} \int_0^\infty \frac{dz\, z^{5/2} e^{-z}}{a - z} = -\left[\frac{3}{4} + \frac{a}{2} + a^2 + a^{5/2} Z(a^{1/2})\right],$$

$$\frac{1}{\sqrt{\pi}} \int_0^\infty \frac{dz\, z^{7/2} e^{-z}}{a - z} = -\left[\frac{15}{8} + \frac{3a}{4} + \frac{a^2}{2} + a^3 + a^{7/2} Z(a^{1/2})\right],$$

where

$$Z(\zeta) = \frac{1}{\sqrt{\pi}} \int_{-\infty}^\infty \frac{dt\, e^{-t^2}}{t - \zeta}$$

is the definition of the plama dispersion function [28] valid for $\operatorname{Im} \zeta > 0$; its analytic continuation is used for $\operatorname{Im} \zeta \leqslant 0$. $f(\lambda)$ and I_1 arise in calculating $\langle \omega_d \rangle / \omega_{d0}$ and can be expressed as

$$f(\lambda) = I_2 + S I_3 - \alpha_c \left(I_4 + \frac{I_1 + I_1'}{2q^2}\right) - \alpha_h \left(I_5 + \frac{1}{2q^2 I_6}\right), \tag{33}$$

with

$$I_1 = \int_0^{\vartheta_T} \frac{d\vartheta}{\sqrt{\cos \vartheta - \cos \vartheta_T}} = \sqrt{2}\, K(k),$$

$$I_1' = \int_0^{\vartheta_T} \frac{d\vartheta}{\sqrt{\cos \vartheta - \cos \vartheta_T}} \frac{1 - \tau}{\tau} \to 0,$$

$$I_2 = \int_0^{\vartheta_T} \frac{d\vartheta \cos \vartheta \sigma / \tau}{\sqrt{\cos \vartheta - \cos \vartheta_T}} \to \sqrt{2}\, [2E(k) - K(k)],$$

$$I_3 = \int_0^{\vartheta_T} \frac{d\vartheta\, \vartheta \sin \vartheta \sigma / \tau}{\sqrt{\cos \vartheta - \cos \vartheta_T}} \to 4\sqrt{2}\, [(k^2 - 1) K(k) + E(k)],$$

$$I_4 = \int_0^{\vartheta_T} \frac{d\vartheta \sin^2 \vartheta \sigma / \tau}{\sqrt{\cos \vartheta - \cos \vartheta_T}} \to \frac{4\sqrt{2}}{3} [(1 - k^2) K(k) + (2k^2 - 1) E(k)],$$

$$I_5 = \int_0^{\vartheta_T} \frac{d\vartheta \sin \vartheta g(\vartheta) \sigma / \tau}{\sqrt{\cos \vartheta - \cos \vartheta_T}},$$

and

$$I_6 = \int_0^{\vartheta_T} \frac{d\vartheta\, p_\perp(\vartheta)}{\sqrt{\cos \vartheta - \cos \vartheta_T}} \frac{1}{\tau}.$$

$E(k)$ and $K(k)$ are the elliptic integrals defined by

$$E(k) = \int_0^{\pi/2} d\gamma (1 - k^2 \sin^2 \gamma)^{1/2},$$

and

$$K(k) = \int_0^{\pi/2} \frac{d\gamma}{(1 - k^2 \sin^2 \gamma)^{1/2}},$$

where $k = \sin(\vartheta_T/2)$. The arrows above indicate that the closed-form expression are valid only in the limit $\sigma = \tau = 1$. In general, these quantities must be computed numerically.

We now describe the boundary conditions to be applied at infinity. The integrations of Eqs. (24) and (25) are started at some large value of ϑ, $\vartheta_m = 2\pi m$, m = integer. The secular term in $h(\vartheta)$ is valuated at ϑ_m,

$$h(\vartheta) \simeq S(\vartheta_m - \vartheta_k) - \alpha_c(\sin \vartheta - \sin \vartheta_k) - \alpha_h [g(\vartheta) - g(\vartheta_k)], \qquad (34)$$

a valid approximation for $|\vartheta - \vartheta_m| < 2\pi$ and $\vartheta_m \gg 2\pi$. Thus, with an error or order $1/\vartheta_m$, the coefficients of the differential equation (24) are purely periodic so that Floquet theory [29] can be applied; the solutions must be of the form

$$\phi(\vartheta) = \hat{\phi}(\vartheta) e^{ik\vartheta}, \qquad (35)$$

with $\phi(\vartheta)$ a function of period 2π, and k some complex constant. Note that k is actually a function of ϑ_m, $k(\vartheta_m)$, as is the function $\hat{\phi}(\vartheta)$. However, in the limit $\vartheta_m \to \infty$, k becomes a constant. This suggests an analogy with WKB theory in which the solution can be expressed in the form

$$\phi(\vartheta) = \hat{\phi}(\vartheta) \exp\left[i \int^{\vartheta} k(\vartheta') \, d\vartheta' \right],$$

where now $\hat{\phi}$ is roughly periodic with period 2π and the changes over larger scale lengths. If we write

$$\int^{\vartheta} k(\vartheta') \, d\vartheta' = \int^{\vartheta_m} k(\vartheta') \, d\vartheta' + \int_{\vartheta_m}^{\vartheta} k(\vartheta') \, d\vartheta',$$

treat the first piece as a constant, and expand $k(\vartheta')$ about ϑ_m, we get

$$\int_{\vartheta_m}^{\vartheta} k(\vartheta') \, d\vartheta' \simeq k(\vartheta_m) \cdot (\vartheta - \vartheta_m) + \frac{(\vartheta - \vartheta_m)^2}{2} \frac{dk(\vartheta_m)}{d\vartheta} + \cdots. \qquad (36)$$

The first term is the piece we pick up in expressing $\phi(\vartheta)$ as in Eq. (35) and provides a local approximaton to the global WKB-like solution at ϑ_m.

To calculate k, we first integrate Eqs. (24) and (25), using Eq. (34) for $h(\vartheta)$, over $\vartheta_{m-} \equiv \vartheta_m - \pi$ to $\vartheta_{m+} \equiv \vartheta_m + \pi$ starting with $\phi(\vartheta_{m-}) = 0$, $(d\phi/d\vartheta)(\vartheta_{m-}) = 1$, and label the resulting values at ϑ_{m+}, $\phi_1 \equiv \phi(\vartheta_{m+})$ $\phi_1' \equiv (d\phi/d\vartheta)(\vartheta_{m+})$. Similarly, we integrate from $\vartheta_{m+} \to \vartheta_{m-}$, with $\phi(\vartheta_{m+}) = 0$, $d\phi(\vartheta_{m+})/d\vartheta = 1$ to get $\phi_2 \equiv \phi(\vartheta_m)$ and $\phi_2' \equiv d\phi(\vartheta_{m+})/d\vartheta$. Using the expression for ϕ given in Eq. (35), it can be shown that

$$k(\vartheta_m) = \frac{i}{2\pi} \ln \left\{ \frac{1}{2}\left(\phi_2' - \phi_2 \frac{\phi_1'}{\phi_1}\right) \pm \frac{1}{2}\left[\left(\phi_2' - \phi_2 \frac{\phi_1'}{\phi_1}\right)^2 + 4\phi_2/\phi_1\right]^{1/2} \right\}, \qquad (37)$$

and we actually obtain two values for $k(\vartheta_m)$. We will be interested in temporally growing modes, so a spatially damped response is generally appropriate, $\text{Im}\, k > 0$. We check to see that this choice also yields outgoing waves, $\text{Re}(\partial\omega/\partial k) > 0$. These two criteria are usually compatible; if they are not, we need a special treatment, as discussed in Section IV and the Appendix. We can then find a value for $d(\ln \phi)/d\vartheta$ at ϑ_{m-}, the boundary condition at infinity, where we need to begin the actual integrations.

At this point, we reintroduce the secular term in $h(\vartheta)$, and go through the procedure previously described to find ϕ_h, the ϕ_i's and q_i's over the range $\vartheta = (2m - 1)\pi$ to $(2m - 3)\pi$. This process is repeated until the origin is reached. We set $\vartheta_k = 0$ and look for even eigenmodes. That is, the boundary condition we enforce at $\vartheta = 0$ is $d(\ln \phi)/d\vartheta = 0$. Odd eigenmodes could also be examined, if desired. The eigenfrequency ω is obtained via a shooting technique. For given ω, Eqs. (24) an (25) are integrated from $\vartheta = \vartheta_m$ to $\vartheta = 0$; $d(\ln \phi)/d\vartheta$ $(\vartheta = 0)$ is then a function of ω. A zero of this function is sought with a secant method. Note that with $\alpha_h = 0$, Eq. (25) reduces to the standard MHD ballooning equation. For this reason, we often start at $\alpha_h = 0$ with a known value of $\omega = i\gamma_{\text{MHD}}$ and increase α_h in small steps using the previous root as a guess for the eigenfrequency at the next point.

To demonstrate the effectiveness of the boundary conditions, we list in Table I the eigenfrequencies of three solutions to Eq. (24) with $\alpha_h = 0$ for various values of m, where $\vartheta_m = 2\pi m$. For case (i), $S = 1$, $\varepsilon = r/R_0 = 0.2$, and $\alpha_c = 0$. This is an example of one of the discrete toroidal eigenmodes that appears in the shear Alfvén continuum when the effects of the variation of magnetic field strength along a field line are included. In particular, the $1/V_A^2$ factor leads to a field line dependence $1/V_A^2 \propto (1 + 2\varepsilon \cos \vartheta)$ in the inertia term; these modes were discussed in detail by Cheng, Chen, and Chance [30]. Note that $\Omega = \omega/\omega_A$ is correct to four decimal places even if $m = 1$. In case (ii) we consider an MHD ballooning root with $S = 0.6$, $\varepsilon = 0.2$, and $\alpha_c = 0.8$. With $m = 2$, we obtain five digits of accuracy and have Ω correct for all digits computed here if $m \geqslant 3$. However, at smaller values of S, the eigenfunctions spread out in ϑ, and the level of accuracy drops somewhat to six-place accuracy. This is seen in case (iii), where $S = 0.2$, $\varepsilon = 0.2$, and $\alpha_c = 0.8$.

TABLE I

m	i	ii	iii
1	0.54047205	0.37101330i	0.14793329i
2	0.54053565	0.36901166i	0.13877013i
3	0.54052609	0.36901026i	0.13826504i
4	0.54052386	0.36901026i	0.13823684i
5	0.54055287	0.36901026i	0.13823475i

III. EXAMPLES FOR DEEPLY TRAPPED PARTICLES

In this section we examine cases in which the particles are confined close to the minimum magnetic field region of the tokamak. For example, this is the sort of distribution that would be introduced by near-perpendicular neutral beam injection. However, perpendicular injection on PDX [31] led to the "fishbone" oscillations [32] which appear to be due to a precessional drift resonance of the energetic particles with the internal kink mode [33]. We will examine the effects these resonances have on high-mode-number ballooning modes in addition to the impact of the energetic particles on the non-resonant MHD ballooning mode.

Some of the parameters required to specify the problem will be fixed. Namely, we set $S = 0.6$, $\alpha_c = 0.8$, $r/R_0 = 0.2$, $r = r_0 + \Delta_r/2$, $q = 2$, $m_i = m_h$, and $q_i = q_h$. These choices were made to aid comparisons with similar theoretical work published previously [17–19]. The remaining parameters are ϑ_0, ω_{a0}/ω_A, and α_h. They will be varied in a systematic fashion to allow us an understanding of how they affect the stability of the system. Note that only ω_{d0}/ω_A involves the mode number n. We can get an idea of what values are reasonable by using PDX-like parameters [31] to estimate ω_{d0}/ω_A and ω_{*0}/ω_{d0}. With $T_i = 3$ keV, $n_i = 3 \times 10^{13}$ cm^{-3}, $B = 2T$,

$$\frac{\omega_{*0}}{\omega_{d0}} \cong (0.28)\left(\frac{100}{T_h/T_i}\right),$$

and

$$\frac{\omega_{d0}}{\omega_A} \cong (0.08)\, n \left(\frac{T_h}{100 \text{ keV}}\right);$$

so that for $n = 10$ and $T_h = 120$ keV, one obtains $\omega_{d0}/\omega_A \cong 1$.

The ratio Δ_r/r was an expansion parameter in the equilibrium calculation; thus we cannot allow it to be too large. In the limit of an infinitely sharp gradient, we have $\Delta_r/r \to 0$, $\hat{P}_{\perp h} \to 0$, but $\alpha_h \neq 0$. Although unrealistic, this limit simplifies the equations significantly. In most instances, we will simply take $\Delta_r/r = 0$ and $\omega_{*0}/\omega_{d0} = 0$. Unlike procedures employed elsewhere [17–19], we will raise α_h from zero, keeping α_c constant.

Figures 1 and 2 show the imaginary and real parts of the eigenfrequency, respectively, as α_h is varied for four values of ω_{d0}/ω_A and $\vartheta_0 = 0.895$: namely, $\omega_{d0}/\omega_A =$ (i) 0.01, (ii) 0.4, (iii) 0.7, and (iv) 2.0. Since ω_{d0}/ω_A is proportional to the energetic particle temperature, and α_h is proportional to the energetic particle pressure, varying α_h at constant ω_{d0}/ω_A implies a change in the hot species density. Case (i) representes the introduction of very low energy, MHD-like, trapped particles. Kinetic effects are small in this case. The increase in the growth rate is due to the increased pressure available to drive the instability; the real part of the frequency is hardly affected at all. Note that the use of the high bounce frequency ordering may be inappropriate for this case; it is included here for purposes of comparison.

Curve (ii) of Figs. 1 and 2 describes the effects of particles with significantly more energy. Their stabilizing effect is seen at small α_h, but is overcome by the destabilizing influence of the drift resonance (Re $\omega \sim \omega_d$) at larger values. Consequently, Im ω increases with α_h for $\alpha_h \gtrsim 1.3$, and Re ω becomes significant compared to ω_d. By further increasing ω_{d0}/ω_A [curve (iii)], the distinction between these two modes becomes clearer. First, we see that we can completely stabilize the MHD ballooning mode (Re $\omega \ll \omega_d$) just before the higher-frequency precessional mode becomes unstable. Note the difference in the real parts of the frequencies for these two modes at $\alpha_h = 1.7$.

Finally, in case (iv) we consider very high energy particles (using the PDX values with a mode number, $n = 10$, this corresponds to $T_h \simeq 240$ keV). We can again completely stabilize the low-frequency root, but now there is some distance in α_h before the other mode becomes unstable. The existence of such a stable window has been noted by others [16, 17]. However, instabilities that we have not considered here may be present inside this window [20, 29].

In those situations where $\omega \ll \omega_d$ and $\vartheta_0 \lesssim \pi/2$, it can be seen that the contribution arising from the kinetic term, Eq. (25), almost exactly cancels the hot particle contribution to the instability drive term in Eq. (24) [17, 19]. Furthermore, as long as α_c is nonzero and ϕ ($\vartheta = 0$) is a local maximum of the eigenfunction, the portion of the kinetic contribution which is not cancelled by the fluid term proportional to α_h counteracts the destabilizing influence of the core pressure piece of the instability drive. Due to the stabilizing shear effects present in a tokamak, the requirements on α_h to do this effectively are not as strict as in a shear-free system such as EBT, where the energetic particle pressure gradient must be sufficient to reverse the local magnetic field gradient.

The high-frequency ($\omega \lesssim \omega_d$) instability is introduced as a result of the negative energy character of the hot particle precessional mode [23] arising out of the kinetic term in Eq. (25). By coupling this mode to positive energy waves or positive dissipation, the negative energy wave can be destabilized; here, the outgoing-wave boundary condition plays the part of positive dissipation [34]. The strength of the coupling is proportional to α_h ($\delta Q \propto \alpha_h$); so, the growth rate of this mode tends to increase as the hot particle pressure gradient is raised.

However, at the same time, the resonant character of the kinetic term provides a
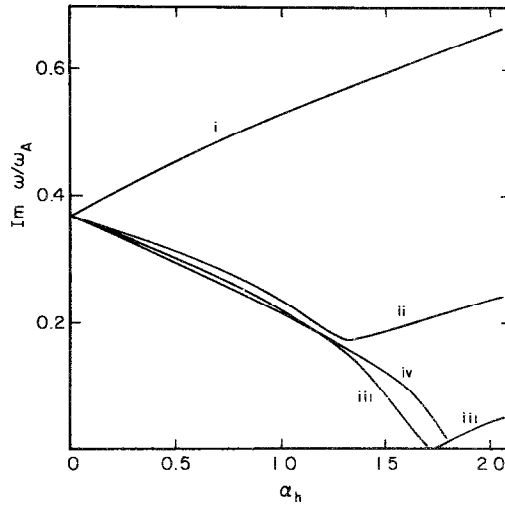
FIG. 1. Imaginary part of the eigenvalue plotted as a function of α_h for four values of the parameter ω_{d0}/ω_A: (i) $\omega_{d0}/\omega_A = 0.01$, (ii) $\omega_{d0}/\omega_A = 0.4$, (iii) $\omega_{d0}/\omega_A = 0.7$, and (iv) $\omega_{d0}/\omega_A = 2$.
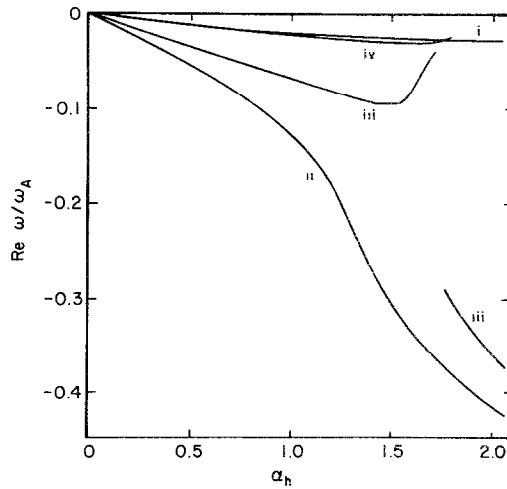

FIG. 2. Real part of the eigenvalue plotted as a function of α_h for four values of the parameter ω_{d0}/ω_A: (i) $\omega_{d0}/\omega_A = 0.01$, (ii) $\omega_{d0}/\omega_A = 0.7$, (iii) $\omega_{d0}/\omega_A = 0.7$, and (iv) $\omega_{d0}/\omega_A = 2$.

source of negative dissipation since $\partial F/\partial \psi < 0$ in the region being studied [35]. The stability of the high-frequency mode is determined by the balance between the positive and negative dissipation. At low energetic particle temperatures, the former depending mostly on properties of the background plasma, prevails and gives rise to instability if α_h is large enough. By raising the energy of the trapped particles, the balance is altered favorably, causing a drop in or even a disappearance of the growth rate.

IV. Study of the Continuous Spectrum

The study of deeply trapped hot particle distributions did not produce any incompatibility in the demands that boundary conditions produce localized modes (i.e., $\lim_{\vartheta \to \infty}((\operatorname{Im} k)/\vartheta) > 0)$ and outgoing waves $(\lim_{|\vartheta| \to \infty} \operatorname{Re}(\vartheta/(\partial \omega/\partial k)) > 0$. However, when sloshing particle distributions are considered, nonlocalized modes are found. For example, when the distribution function in Eq. (22) is chosen, the search for eigenvalues gives the results shown in Fig. 3. The parameters for curve (i) are $\Delta\lambda = 0.02$, $\vartheta_0 = 3.04$, $\omega_{d0}/\omega_A = 0.636$, and $\omega_{*0}/ = \omega_{d0} = 0$; in curve (ii), they are the same except that $\omega_{*0}/\omega_{d0} = 0.55$. Eigenvalues are obained for $\alpha_h < \alpha_{h,cr}$; in this range the two boundary conditions stated above are compatible [$\alpha_{h,cr} \simeq 1.2$ for curve (i) and $\alpha_{h,cr} \simeq 2.2$ for curve (ii); the apparent touching of the two curves at $\alpha_h = 1.2$ is accidental]. However, when $\alpha_h \gtrsim \alpha_{h,cr}$, the eigenmode no longer satisfies the outgoing wave and mode localization conditions simultaneously.

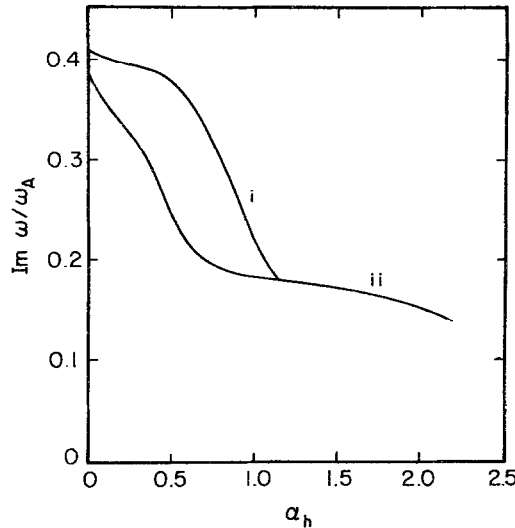Fig. 3. Imaginary part of the eigenvalue plotted as a function of α_h for $\Delta\lambda = 0.02$, $\vartheta_0 = 3.04$, and (i) $\omega_{*0}/\omega_{d0} = 0$, (ii) $\omega_{*0}/\omega_{d0} = 0.55$.

From physical considerations we expect that the outgoing wave condition, which is amplifying at infinity, is the physically correct condition. This statement will be further justified below. However, instead of studying the difficult problem of finding waves that amplify at infinity (this procedure is sensitive to small numerical errors), we can study the stability of the continuum modes directly. These modes have the property that at infinity the wavenumber k is purely real. It can be shown that if the continuum modes are stable, then an unstable global mode must be spatially localized. But if the continuum modes are unstable, we shall show that it is possible for the global modes to be spatially amplifying at infinity [34]. Thus, if one is attempting to find a stable set of equilibrium parameters, one must first stabilize the continuous spectrum, and then examine the stability of the global eigenmodes.

Before discussing the continuum modes, we will justify why spatially growing outgoing waves at infinity can be an appropriate boundary condition for discrete eigenmodes. First of all, for simplification let us consider a system, with, say, an independent variable x, that is described by a linear spatially inhomogeneous integral operator $\hat{D}_{x,t}^{SI}$ that asymptotically approaches a linear spatially homogeneous operator, $\hat{D}_{x,t}^{SH}$ as $|x| \to \infty$. The eigenvalue problem for an eigenfunction $\phi_1(x) e^{-i\omega t}$ (the $\exp(-i\omega t)$ dependence of the eigenfunction is guaranteed from the linearity of the equation) is determined from the solution of the equation

$$\hat{D}_{x,t}^{SI} \cdot \phi_1(x) e^{-i\omega t} = 0. \tag{38}$$

This equation can be rewritten as

$$\hat{D}_{x,t}^{SH} \cdot \phi_1(x) e^{-i\omega t} = S_{x,t}^{SH}, \tag{39}$$

where

$$S_{x,t}^{SH} = (\hat{D}_{x,t}^{SI} - \hat{D}_{x,t}^{SH}) \phi_1(x, t) e^{-i\omega t}. \tag{40}$$

Now, using Eq. (38), $S_{x,t}^{SH}$ has the property that it vanishes as $|x| \to \infty$ as then $\hat{D}_{x,t}^{SI} \to \hat{D}_{x,t}^{SH}$. Thus $S_{x,t}^{SH}$ can be viewed as a spatially bounded source function of frequency ω that excites a physical system characterized by a spatially homogeneous operator $\hat{D}_{x,t}^{SH}$. We shall assume that this excitation and the solution is consistent with causality constraints that typically arise in initial value problems (with causality taken into account the solution $\phi_1'(x, t) \exp(-i\omega t)$ is valid only as $t \to \infty$).

The eigenfunctions of $\hat{D}_{x,t}^{SH}$ are plane waves

$$\phi_{SH} = \exp(ikx - i\omega t) \tag{41}$$

with k real. However, if the operator $D_{x,t}^{SH}$ leads to unstable waves, then solutions with $\text{Im } \omega > 0$ can be found with real k. If in such a system, excitation is supplied by a localized source (such as in Eq. (40)), with another frequency, say ω_0, then spatially amplifying solutions of the form of Eq. (41) with $x \, \text{Im } k < 0$ are possible as $|x| \to \infty$. These solutions are the spatially asymptotic form of convective and absolute waves [36, 37]. Thus, $\phi_1(x) \to \exp(ikx)$ with, in general, k complex. The

exact criterion for when one has spatially amplifying waves is somewhat more complicated than stated above, and is discussed in detail in the Appendix and summarized in the conclusion. A simplified criterion that is usually correct will be stated shortly in this section.

For the problem considered in this paper we have to modify our arguments somewhat to pose the boundary value problem; our operator defined in Eqs. (4) and (5) has the same property as the class of operators $\hat{D}_{x,t}^{\text{SI}}$ that asymptotically approach a spatially periodic operator as the independent variable $|x| \to \infty$, i.e.,

$$\lim_{|x| \to \infty} \hat{D}_{x,t}^{\text{SI}} = \hat{D}_{x,t}^{\text{SP}}.$$

From the Floquet theorem [25], the eigenfunctions of the spatially periodic operator, $\hat{D}_{x,t}^{\text{SP}}$, are of the form

$$\phi_k(x) \exp(-i\omega t + ikx), \tag{42}$$

where $\phi_k(x)$ is a periodic function and k is real. Now, as with the case in Eqs. (38)–(40), the eigenvalue problem for the eigenfunction ϕ_2 can be formulated as

$$\hat{D}_{x,t}^{\text{SP}} \cdot \phi_2(x) e^{-i\omega t} = S_{x,t}^{\text{SP}}$$

with

$$S_{x,t}^{\text{SP}} = (\hat{D}_{x,t}^{\text{SP}} - \hat{D}_{x,t}^{\text{SI}}) \phi_2(x) e^{-i\omega t}.$$

As before, $S_{x,t}^{\text{SP}}$ can be viewed as a spatially bounded source function. In the Appendix we show that $\phi_2(x)$ will asymptotically approach the form of Eq. (42) with k complex and perhaps even with spatial amplification ($x \operatorname{Im} k < 0$) if $\operatorname{Im} \omega > 0$ for k real. The precise criterion for finding spatially amplifying waves is given in the Appendix and summarized in the Conclusion, with a simplified criterion given below.

Now, using the results of the Appendix, we conclude the following. First of all, suppose the operator $\hat{D}_{x,t}^{\text{SI}}$ approaches a spatially homogeneous operator for large $|x|$, and one finds $\operatorname{Im} \omega(k) > 0$ for a real band in k. We classify such a case as continuum instability. Asymptotically, for large $|x|$, this instability can be convective or absolute [36, 37]. In a convective instability the response to a spatially localized, temporally bounded source will be spatially growing but temporally bounded at a fixed spatial point. The typical response for x large and positive is $\exp[ikx - i\omega(k)\,t]$ with $\omega(k)$ real, $\operatorname{Re}(\partial\omega/\partial k) > 0$, and $\operatorname{Im} k < 0$ ($\partial\omega/\partial k \equiv v_g \equiv$ group velocity). In an absolute instability the response at a given spatial point is unbounded in time. The characteristic frequency response of an absolute instability occurs where $\partial\omega(k)/\partial k = 0$ (or equivalently where k has a double root as a function of ω) and $\operatorname{Im} k \leqslant 0$ as $x \to +\infty$. Furthermore, if an oscillator is applied at an external complex frequency ω_0 with $\operatorname{Im} \omega_0 > \operatorname{Im} \omega(k)$ for all real k, then the spatial response of waves propagating away from the source decays, i.e., as $x \to \infty$ the perturbed

response is of the form $\exp[ik(\omega_0) t]$, with $\operatorname{Im} k(\omega_0) > 0$ and $\operatorname{Re} v_g > 0$. If $\operatorname{Im} \omega_0 < \operatorname{Im} \omega(k)$, then k should be chosen so that $x \operatorname{Re} v_g > 0$, and this can lead to spatially amplifying solutions where $x \operatorname{Im} k < 0$ (these statements are a somewhat simplified version of the exact criterion given in the Appendix). For a discrete eigenvalue ω_0, the eigenfunction at infinity has the same structure as the response to a bounded externally imposed oscillator.

In a periodic equilibrium, the eigenfunctions of the system are of the form

$$\phi_k(x) \exp[ikx - i\omega(k) t],$$

with k a real continuous parameter and $\phi_k(x)$ a periodic function of x. In the Appendix we show that the nature of convective and absolute instabilities and their amplification and attenuation response to externally spatially bounded oscillators are entirely the same for periodic systems as for spatially homogeneous systems. Thus, the criteria for selecting the boundary conditions at infinity is the same as the asymptotically spatially homogeneous case.

Now, we apply the above discussion to the specific problem of this paper. We note that the asymptotic operator that we are considering (now the independent variable is θ) at large ϑ in Eqs. (24) and (25) is spatially periodic. Thus, this operator is in the class of operators having Floquet-type eigenfunctions, and we can classify the continuum modes as being convectively or absolutely unstable. We observe that in attempting to find a global eigenfunctions of Eqs. (4) and (5) with a discrete eigenvalue, choosing a guess $\omega = \omega_0$ is equivalent to applying to the asymptotic operator a source with a frequency ω_0. If $\operatorname{Im} \omega_0 > \operatorname{Im} \omega(k)$ for real k, we are guaranteed a response as $\vartheta \to \infty$ in which the conditions $\operatorname{Im} k > 0$ and $\operatorname{Re} v_g > 0$ are compatible. However, if $\operatorname{Im} \omega_0 < \operatorname{Im} \omega(k)$ for some k, there need not be a compatibility of the two types of boundary conditions. By observing the response of a convective instability to a localized source as we analyze in the Appendix, we can ascertain that the boundary condition $\operatorname{Re} v_g > 0$ as $\vartheta \to \infty$ is the correct one (this criterion is strictly correct only if $\operatorname{Im} k \ll \operatorname{Re} k$).

There may be some criticism of the form of eigenfunction and eigenvalue we are considering. Our eigenvalues that are obtained by our procedure are somewhat analogous to the classic eigenvalues giving rise to Landau damping [38]. The most narrowly defined eigenvalue problem gives rise to the continuum Case–Van Kampen modes [39, 40], and the Landau solution is a superposition of Case–Van Kampen modes. Nonetheless, the Landau solution is a commonly accepted and useful formulation of the eigenvaue problem. Another form of criticism is that the eigenfunction of a tokamak does not really go to a spatially remote region, but continually returns to the same place because of spatial periodicity in the toroidal and poloidal directions. Then an amplifying wave would eventually nonlinearly saturate, giving rise to an entirely different response than the linear theory prediction. To respond to this point, we note that the operator in Eqs. (4)–(5) is in fact physically incomplete in the limit of large θ. In a more exact ballooning mode theory, where the Larmor radius is finite, Larmor radius effects

profoundly change the nature of the solution at infinity. As the radial wavenumber continually increases in a system with magnetic shear, when all the finite Larmor radius effects are taken into account the mode ultimately propagates to a region which is locally stable (i.e., the WKB theory along the field line is stable for real k). There is an implicit assumption in our formulation that the solution between the asymptotically far region described by Eqs. (4) and (5) and the even further outer region where plane waves are locally stable, can be described by a WKB theory along the field lines that does not give rise to additional wave reflection. Further, investigations of the detailed problem may be needed to confirm this assumption. Numerical work in a related problem where amplifying outgoing waves were taken in the region that can be described by WKB theory, but where local stabilization occurs at spatial regions yet further away, confirmed that the boundary condition was accurate if the local WKB theory did not fail in the intermediate region [41].

In any event, even if one refuses to accept the spatially amplifying eigenfunctions of Eqs. (4) and (5) as being physically or mathematically acceptable because of the uncertainty of whether WKB theory always applies where these equations fail, or for other reasons, the need to examine the stability of the continuum solutions of Eqs. (4) and (5) is still valid. If the continum solutions are stable, there is no problem in using conventional localized boundary conditions for ballooning modes. If they are unstable, we know we have an unstable continuous spectrum, as well as a possible discrete spectrum with lower growth rates, with spatial amplification at large distances along the field line. Because of the spatial amplification, this discrete mode may be somewhat difficult to determine numerically. However, the stability search is simplified by examining the eigenvalues for the continuous spectrum of the asymptotic operator. If it is possible to alter the parameters so that the continuous spectrum of the asymptotic operator is completely stable, then we are guaranteed that an unstable global eigenfunction must be localized in space. Thus, in order to find parameters that completely stabilize the system, it is first necessary to stabilize the set of asymptotic equations.

The numerical search of the continuous spectrum was performed for the two sloshing ion distributions given in Eqs. (22) and (23). The search for eigenvalues is made as follows. We look for eigenfunctions of Eqs. (24) and (25) in the limit $\vartheta \to \infty$. In this case, the asymptotic form of the governing equations is

$$\frac{d}{d\vartheta} \sigma \frac{d\phi}{d\vartheta} + \frac{\omega^2}{\omega_A^2} \phi = -\sin \vartheta \sigma q r R_0 \, \delta Q \tag{43}$$

and

$$\sigma \, \delta Q = m_h \int d^3 v \frac{\omega - \omega_*}{\omega - \langle \omega_d \rangle} \mu^2 \frac{\partial F_h}{\partial E} \left[\langle \delta Q \rangle + \frac{q}{r R_0} \left\langle \frac{\sigma}{\tau} \phi \sin \vartheta \right\rangle \right], \tag{44}$$

where for simplicity we have neglected $2\varepsilon \cos \vartheta$ and ω_{*i} in the inertia term. We note from the symmetry of these equations that coupling between ϕ and δQ only occurs

if ϕ is odd and δQ is even. The symmetry also implies that $\omega(-k)=\omega(k)$ and $\omega(k+1)=\omega(k)$. From these conditions it follows that $\partial\omega(k)/\partial k=0$ for $2k=$ integer. We also observe that two independent solutions for ϕ are obtained by construction of $\phi_1(\vartheta)$ and $\phi_2(\vartheta)$ with the boundary conditions

$$\varphi_1(-\pi)=0, \qquad \frac{d\varphi_1}{d\vartheta}(-\pi)=1,$$

$$\varphi_2(\pi)=0, \qquad \frac{d\varphi_2}{d\vartheta}(\pi)=1.$$

From the symmetry of Eq. (43), it is clear that $\varphi_1(\vartheta)=-\varphi_2(-\vartheta)$ and $d\varphi_1(\vartheta)/d\vartheta = d\varphi_2(-\vartheta)/d\vartheta$. Now, an eigenfunction $\varphi(\vartheta)$ of the system must have the properties

$$\varphi(\vartheta+2\pi)=\varphi(\vartheta)\exp(2\pi ik), \qquad \frac{d\varphi}{d\vartheta}(\vartheta+2\pi)=\frac{d\varphi}{d\vartheta}(\vartheta)\exp(2\pi ik)$$

and

$$\varphi=\varphi_1(\vartheta)+A\varphi_2(\vartheta)\equiv\varphi_1(\vartheta)+A\varphi_1(-\vartheta).$$

It is straightforward to show that $A=\exp(-2\pi ik)$ and $\varphi_1(\pi)=\cos(2\pi k)$. Thus, in searching for the eigenvalues $\omega(k)$ we iterate as follows. We guess a value for ω, integrate Eqs. (24) and (25) in the limit $h\to\infty$ with the boundary condition $\varphi_1(-\pi)=0$, $d\varphi_1(-\pi)/d\vartheta=1$ to $\vartheta=\pi$, and alter ω until the condition $\varphi_1(\pi)=\cos 2\pi k$ is fulfilled.

In this search, we find that these continuum modes are unstable. The most unstable modes for the distribution function in Eq. (22) are at the pinch point $k=0$, while the most unstable modes for the distribution function in Eq. (23) are at the pinch point $k=\frac{1}{2}$.

$\vartheta_0=3.04$. The reduction in growth rate at small values of $\Delta\lambda$ is the result of a decreasing contribution to the kinetic integral in Eq. (25) by the resonant $(\omega_*\langle\omega_d\rangle>0)$ particles that give the equation a nonzero imaginary part and therefore a complex ω. Unfortunately, the value of $\Delta\lambda$ required to stabilize the $k=0$ continuum mode is too small to give rise to a physically realizable distribution.

We present the results of calculating ω for the $k=\frac{1}{2}$ mode as a function of α_h in Fig. 5 using the distribution in Eq. (23). In this case, we have set $\Delta\lambda=0.02$, $\omega_{d0}/\omega_A=5$, and $\alpha_c=0$. An interesting feature of this mode is that it is almost purely growing at large α_h. There are very few resonant particles in this instance so that the kinetic integral is mostly real; however, its sign is such that it leads to nearly purely growing instabilities. On the other hand, at small α_h the number of resonant particles increases and the energetic particle response becomes complex so that the
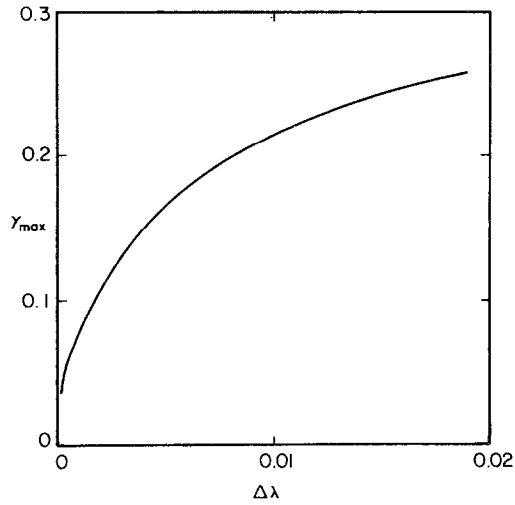
FIG. 4. Plot of $\gamma_{max} = \mathrm{Im}\ \omega/\omega_A$ as a function of $\Delta\lambda$ for the $k = 0$ mode with $\alpha_h = 1.52$ using the purely trapped distribution given in Eq. (22).
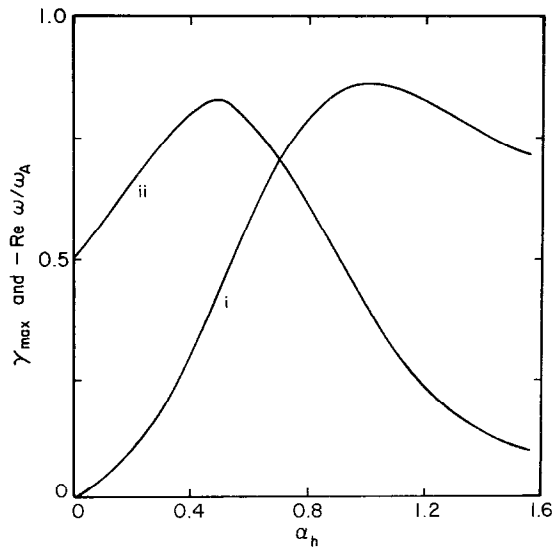

FIG. 5. Plot of $\gamma_{max} = \mathrm{Im}\ \omega/\omega_A$ and the negative of the real part of the frequency for the $k = \frac{1}{2}$ mode using the trapped and circulating distribution given in Eq. (23), with $\Delta\lambda = 0.02$, $\omega_{d0}/\omega_A = 5$, and $\alpha_c = 0$.

mode frequency obtains a significant real part, with the frequency approaching $-\omega_A/2$ as $\alpha_h \to 0$. In this region, the $k = \frac{1}{2}$ mode is similar in behavior to the $k = 0$ mode discussed above.

V. Conclusion

In this paper we have developed numerical methods for solving the ballooning mode MHD equation when modified with the inclusion of trapped hot particles treated in the high bounce frequency limit.

One of the novel aspects of the work was to show that in certain cases it is necessary to modify the conventional evanescent boundary conditions for the eigenfunction and allow for exponentially growing waves at infinity. This arises in the following situation. As the magnitude of the poloidal angle $|\theta| \to \infty$, the integrodifferential operator describing the mode becomes periodic in θ, allowing an asymptotic solution of the eigenfunction of the form

$$\phi_k(\theta)\exp(ik\theta),$$

where $\phi_k(\theta)$ is a periodic function. Now, suppose the asymptotic spatially periodic operator, denoted as $\hat{D}_x^{SP}(\omega)$, allows an unstable solution in ω for real k. In Fig. 6b we indicate $\omega(k)$ (for k real) by the solid curve between P_1 and P_2. If we seek a discrete eigenvalue ω_0 that lies underneath this curve, then the boundary conditions at large $|\theta|$ restrict the choice of k so that it is amplifying in space (i.e., $\theta \operatorname{Im} k < 0$). Usually, this choice also implies that $\theta \operatorname{Re} v_g > 0$ ($v_g \equiv$ group velocity), although this latter conclusion only strictly applies if $|\operatorname{Im} k| \ll |\operatorname{Re} k|$.

If ω_0 lies outside the curve $\omega(k)$ (for k real) then the usual evanescent boundary condition applies for the eigenfunction (i.e., $\theta \operatorname{Im} k > 0$). From these observations it is clear that when searching for stability it is necessary to find parameters where the continuum mode is stable, i.e., $\operatorname{Im} \omega(k) \leq 0$ for all real k. Only then is the discrete unstable spectrum guaranteed to have eigenfunctions that decay at infinity.

In addition to establishing the boundary conditions, we have developed a new WKB technique for almost spatially periodic systems. This theory makes the search for eigenvalues more efficient as one then does not have to integrate from too large a value of θ to find eigenfunctions and eigenvalues accurately.

The detail method of solution of the integrodifferential equations governing hot particle ballooning modes is explained in detail in the text. Sample solutions are shown. The purpose of this paper was to discuss some of the rather novel numerical aspects of this problem. For a more detailed discussion of the physical aspects of the problem the reader is referred to Ref. [22].

APPENDIX: BOUNDARY CONDITIONS FOR WAVES IN
SPATIALLY HOMOGENEOUS AND SPATIALLY PERIODIC EQUILIBRIA

We wish to modify the theory of convective and absolute instabilities in a spatially homogeneous system [37, 38] and extend the result to the response of waves in a periodic system. The purpose of this discussion is to understand the boundary condition needed for the integral equations examined in the text; this system asymptotically approaches one that can be described by an operator with periodic symmetry.

We shall represent an operator characterizing the response to linear perturbations by the symbol $\hat{D}_{x,t}$. In a spatially homogeneous system, this linear operator exhibits invariance to arbitrary space and time translations, so that

$$\hat{D}_{x+L \cdot t+T} = \hat{D}_{x,t} \tag{A.1}$$

for arbitrary L and T. From this property it follows that the eigenfunctions for the system must be of the form

$$\exp[ikx - i\omega(k)\, t], \tag{A.2}$$

where k is real, and for a given k, multiple complex $\omega(k)$ exist. If $\operatorname{Im} \omega(k) > 0$, the system is linearly unstable. We shall use the superscript SH (spatially homogeneous) to denote the class of operators satisfying Eq. (A.1).

In periodic equilibria of period L_0, the linear response operator (now denoted with a superscript SP for spatially periodic) has the symmetry property

$$\hat{D}^{SP}_{x+nL_0,t+T} = \hat{D}^{SP}_{x,t} \tag{A.3}$$

for arbitrary T and any integer n. Given the symmetry shown in Eq. (A.3) it follows from Floquet theory that the eigenfunctions of $\hat{D}^{SP}_{x,t}$ are of the form

$$\phi_{k,n}(x) \exp[ikx - i\omega_n(k)\, t], \tag{A.4}$$

where $\phi_{k,n}(x + L_0) = \phi_{k,n}(x)$, k is real, and the n-index indicates the multiple values of $\phi_{k,n}(x)$ and $\omega_n(k)$ for a given k.

Now let us develop the theory for the response of a spatially homogeneous system to a localized source in a manner similar to that used in Ref. [38]. We need to obtain the asymptotic solution to the equation

$$\hat{D}^{SH}_{x,t}\psi(x, t) = \hat{S}(x)\, H(t) \exp(-i\omega_0 t); \qquad H(t) = 1, \quad t > 0$$
$$= 0, \quad t < 0, \tag{A.5}$$

$$\lim_{\substack{|x| \to \infty \\ \operatorname{Im} \omega_0 > 0}} \frac{\hat{S}(x)}{|x|^m} \to 0$$

for all m. By taking the spatial Fourier and the temporal Laplace transforms of Eq. (A.5), we find the solution

$$\psi(x, t) = i \int_{-\infty}^{\infty} \frac{dk}{2\pi} \int_{C(\omega)} \frac{d\omega}{2\pi} \frac{S(k) \exp[-i\omega t + ikx]}{(\omega - \omega_0) D^{\mathrm{SH}}(k, \omega)}, \qquad (A.6)$$

where

$$S(k) = \int_{-\infty}^{\infty} dx \exp(-ikx) \hat{S}(x),$$

$$D^{\mathrm{SH}}(k, \omega) = \int_0^{\infty} dt \int_{-\infty}^{\infty} dx \exp[-ikx + i\omega t] \hat{D}_{x,t}^{\mathrm{SH}}. \qquad (A.7)$$

$C(\omega)$ is a contour in the ω plane above all the zeros of the denominator which are ω_0 and $\omega(k)$ with $D^{\mathrm{SH}}(k, \omega(k)) = 0$ (see Fig. 6).

We shall assume that $\operatorname{Im} \omega(k) > 0$ for some bands of k. The contour $\tilde{C}(\omega(k))$, shown in Fig. 6(a), is the map of real k onto the complex ω plane in regions where
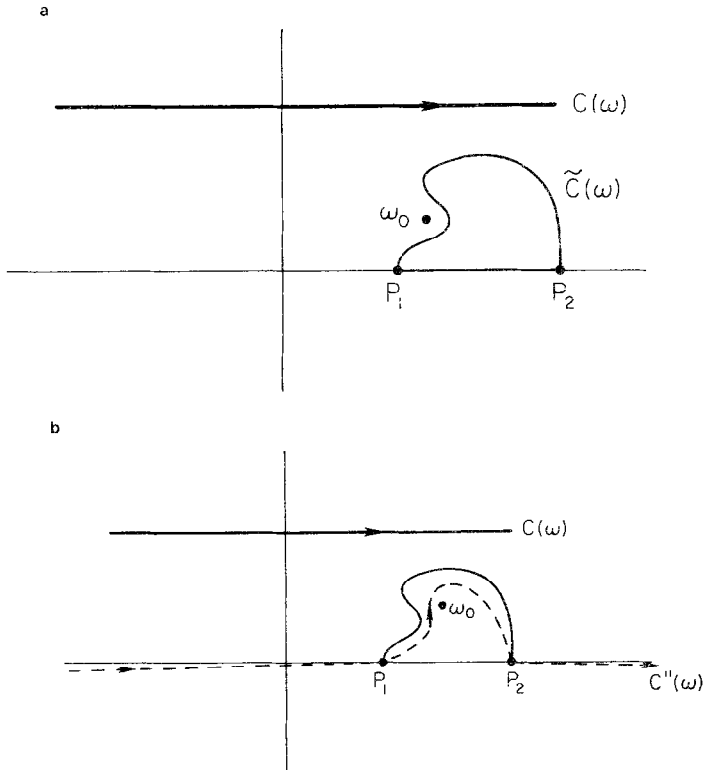

FIG. 6. Original $C(\omega)$ contour that must lie above $\omega = \omega_0$ and $\omega = \omega(k)$. The contour $\tilde{C}(\omega)$ represents $\omega = \omega(k)$ for real k. In (a) ω_0 lies outside $\tilde{C}(\omega)$ and in (b) ω_0 lies inside $\tilde{C}(\omega)$. The contour $C''(\omega)$ is the contour of integration in Eq. (A.17).

Im $\omega(k) > 0$. The end-points P_1 and P_2, at $k = k_1$ and $k = k_2$, respectively, are where Im $\omega(k_{1,2}) = 0$. Usually there are several such contours arising from bands of real k where Im $\omega > 0$. A frequent case is where $\omega(k) = \omega(-k)$. In this case the two $\tilde{C}(\omega)$ contours are identical, but as real k increases, one of the contours maps in the clockwise direction, while the other maps in the counterclockwise direction. In general, a given $\tilde{C}(\omega)$ contour winds in either the clockwise direction or the counterclockwise direction. Now

$$\frac{d\omega}{dk} = \frac{-\dfrac{\partial D}{\partial k}}{\dfrac{\partial D}{\partial \omega}} \equiv v_g,$$

where v_g is the group velocity, and Re $\delta\omega = \delta k$ Re v_g, where δk and $\delta\omega$ are incremental changes in ω and k. Thus, as k increases, a clockwise (counterclockwise) contour of $\tilde{C}(\omega)$ has Re v_g predominantly positive (negative). We shall assume that $v_g \neq 0$ on $\hat{C}(\omega)$, with the possible exception of the end-points. However, Re v_g can change sign. For example, if we assume $\tilde{C}(\omega)$ in Fig. 6b is a clockwise contour, there is a small region where Re $\omega(k_2) >$ Re $\omega(k_1)$ for $k_2 > k_1$. Hence, though the predominant sign of Re v_g is positive, in the region where Re ω doubles back, Re $v_g < 0$. We shall define $\text{sg}(\tilde{C}) = 1$ if the contour is clockwise and $\text{sg}(\tilde{C}) = -1$ if the contour is counterclockwise.

A frequency ω_0 is defined to be inside the bounter $\tilde{C}(\omega)$ if it lies between $\tilde{C}(\omega)$ and the real axis. Otherwise ω_0 is outside this contour.

Suppose for definiteness that the contour $\tilde{C}(\omega)$ is clockwise, and we distort $\omega(k)$ to move inside the contour towards the real axis between P_1 and P_2. Because of the clockwise assumption, $\tilde{C}(\omega)$ goes from P_1 to P_2 and Re v_g is predominantly positive. Now let $\omega(k) \rightarrow \omega(k) - i\varepsilon$ with ε real. δk, the change of k, is found from the dispersion relation as

$$\delta k = -i\varepsilon/v_g, \tag{A.8}$$

so that

$$\text{Im } \delta k = -\frac{\varepsilon}{|v_g|^2} \text{ Re } v_g. \tag{A.9}$$

From Fig. 6a it is clear that to go to the inside of $\tilde{C}(\omega)$ requires $\varepsilon > 0$ if Re $v_g > 0$ (as then Re ω increases with increasing k) and $\varepsilon < 0$ if Re $v_g < 0$ (as then Re ω decreases with increasing k as illustrated by the small segment of the $\tilde{C}(\omega)$ above $\omega = \omega_0$). In any case, it follows from (A.9) that to go to the inside of $\tilde{C}(\omega)$ requires

a clockwise contour $\tilde{C}(\omega)$ have Im $k < 0$. Similar arguments hold for counterclockwise contours. Thus, we conclude that all $k(\omega)$ points on the inside of clockwise (counterclockwise) $\tilde{C}(\omega)$ contours have Im $k < 0$ (Im $k > 0$) and produce spatial amplifications towards the positive (negative) x-direction.

Now, suppose ω_0 in Eq. (A.6) lies outside the contours $\tilde{C}_j(\omega)$ (the subscript j specifies the set of possible contours) as shown in Fig. 6a. Then to evaluate the dominant response of Eq. (A.6) we bring the C-contour down to the real axis. In so doing we pass the poles at $\omega = \omega_0$ and $\omega = \omega_j(k)$, where $D(k, \omega_j(k)) = 0$ and $\operatorname{Im} \omega_j(k) > 0$. Thus, $\psi(x, t)$ becomes

$$\psi(x, t) = \int_{(\text{real } k)} \frac{dk}{2\pi} \frac{S(k) \exp[-i\omega_0 t + ikx]}{D^{\text{SH}}(k, \omega_0)} + \sum_j \int \frac{dk}{2\pi} \frac{S(k) \exp[-i\omega_j(k) t + ikx]}{(\omega - \omega_0) \frac{\partial}{\partial \omega} D^{\text{SH}}(k, \omega_j(k))}$$

$$+ i \int_{\text{real } k} \frac{dk}{2\pi} \int_{C'(\omega)} \frac{d\omega}{2\pi} \frac{S(k) \exp[-i\omega t + ikx]}{(\omega - \omega_0) D^{\text{SH}}(k, \omega)}, \tag{A.10}$$

where $C'(\omega)$ is on the real ω-axis. The first and second terms have exponential factors that amplify with time, while the last integral is bounded in time. Therefore, the last term can be ignored when compared with the other two. In the second term we make the dispersion transformation from k to ω through the dispersion relation $D^{\text{SH}}(k, \omega) = 0$ for k in the interval $k_{1j} < k < k_{2j}$. Then using

$$\frac{d\omega}{dk} = -\frac{\partial D^{\text{SH}}(k, \omega(k))}{\partial k} \bigg/ \frac{\partial D^{\text{SH}}(k, \omega(k))}{\partial \omega}.$$

the dominant temporal response to Eq. (A.10) can be written as

$$\psi(x, t) = \psi_1(x, t) + \psi_2(x, t) \tag{A.11}$$

with

$$\psi_1(x, t) = \int_{\text{real } k} \frac{dk}{2\pi} \frac{S(k) \exp[-i\omega_0 t + ikx]}{D^{\text{SH}}(k, \omega_0)} \tag{A.12}$$

$$\psi_2(x, t) = -\sum_j \int_{\tilde{C}_j} \frac{d\omega}{2\pi} \frac{S(k(\omega)) \exp[-i\omega t + ik(\omega) x]}{(\omega - \omega_0) \frac{\partial D^{\text{SH}}(k, \omega(k))}{\partial k}}. \tag{A.13}$$

In evaluating the first integral for $x > 0$ ($x < 0$), we need to distort the contour in the upper (lower) k plane towards infinity. As we distort we may encounter a pole at $k = k_{0j}$ where $D^{\text{SH}}(k_{0j}, \omega_0) = 0$. These poles give rise to spatially damped contributions to Eq. (A.12). Thus, assuming that $S(k)$ has no singular points, we find

$$\psi_1(x, t) = i \sum_{\substack{j \\ (x \operatorname{Im} k_j > 0)}} \frac{\exp[ik_{0j}x - i\omega_0 t] S(k_{0j}) \operatorname{sg}(x)}{\frac{\partial D^{\text{SH}}(k_{0j}, \omega_0)}{\partial k}}$$

$$+ \int_{C_k} dk \frac{S(k) \exp[ikx - i\omega_0 t]}{D^{\text{SH}}(k, \omega_0)}, \tag{A.14}$$

where C_k contour is shown in Fig. 7 for $x > 0$; we have assumed possible non-analytic points at $k = 0$ and $k = \pm k_e$. For this discussion we ignore the contribution from these nonanalytic points (although physically they may be quite important) and emphasize the pole contributions at k_{0j}.

To evaluate $\psi_2(x, t)$ we distort the ω contour to the real axis. Since ω_0 is assumed to be outside $\tilde{C}(\omega)$, there are no poles from $\omega = \omega_0$. However, we may encounter branch points where $\partial D^{SH}(k_b, \omega_b)/\partial k$ and $D^{SH}(k_b, \omega_b)$ vanish. If such points exist the $\tilde{C}(\omega)$ contour cannot be completely deformed to the real ω-axis, but must wind around the points ω_{bj}. Thus in Fig. 8a, the $\tilde{C}(\omega)$ contour is distorted to be along the real axis, except where it needs to rise and fall to go around $\omega = \omega_{bj}$. Then the typical response for $t \to \infty$ can be evaluated by integrating near the branch points ω_{bj} by the method of stationary phase to give

$$\psi_2(x, t) = \sum_j \frac{S(k_{bj}) \exp[ik_{bj}x - i\omega_{bj}t]}{(iD_{kk}^{SH} D_{\omega}^{SH} t)^{1/2}(\omega_{bj} - \omega_0)}. \tag{A.15}$$

Thus, the characteristic response to $\psi(x, t)$ for long times is

$$\psi(x, t) = i \sum_{\substack{j \\ (x \operatorname{Im} k_{0j} > 0)}} \frac{\exp[ik_{0j}x - i\omega_0 t] S(k_{0j}) \operatorname{sg} x}{\dfrac{\partial D^{SH}(k_{0j}, \omega_0)}{\partial k}}$$

$$+ \sum_j \frac{S(k_{bj}) \exp[ik_{bj}x - i\omega_{bj}t]}{[iD_{kk}^{SH}(k_{bj}, \omega_{bj}) D_{\omega}^{SH}(k_b, \omega_{bj}) t]^{1/2}(\omega_{bj} - \omega_0)}. \tag{A.16}$$

There are several important conclusions that follow from these results:

(1) If ω_0 is outside $\tilde{C}(\omega)$, $x \operatorname{Im} k_j > 0$, which causes attenuation in the direction of increasing $|x|$.
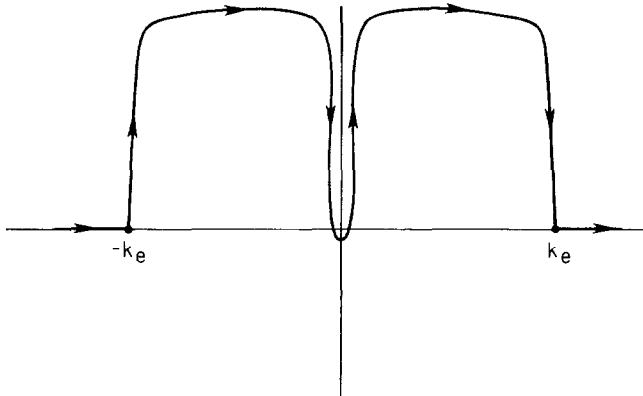

FIG. 7. The contour C_k, distorted away from the real axis into the upper half-plane of $\chi > 0$.
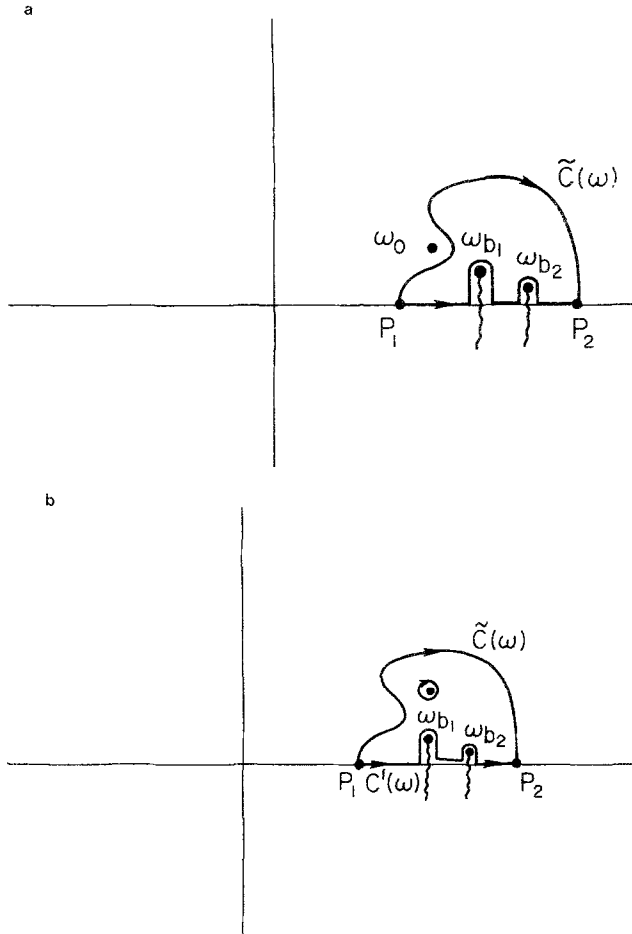
a

b

FIG. 8.   The distortion of the $\tilde{C}(\omega)$ contour where ω is complex and k is real to the real ω axis or to a steepest descent contour. In (a) ω_0 lies outside $\tilde{C}(\omega)$ and in (b) ω_0 lies inside $\tilde{C}(\omega)$.

(2) If $\tilde{C}_j(\omega)$ is a clockwise (counterclockwise) contour so that $\mathrm{Re}\, v_g$ is predominantly positive (negative) for real k $\mathrm{Im}\, k_{bj} < 0$ ($\mathrm{Im}\, k_{bj} > 0$), it leads to amplification in the positive (negative) x-direction and decay in the negative (positive) x-direction.

(3) The characteristic frequency response in Eq. (A.16) comes from the term with the largest $\mathrm{Im}\, \omega$.

Now let us assume ω_0 is inside some of the $\tilde{C}_j(\omega)$ contours as shown in Fig. 6b. We evaluate as indicated above the contributions from those contours $\tilde{C}_j(\omega)$ in which ω_0 is on the outside. The contributions in which ω_0 is on the inside are evaluated as follows. We lower the appropriate $\tilde{C}_j(\omega)$ contours so that they pass

through all poles of $\omega(k)$ but still lie above ω_0. The contribution to Eq. (A.6) from those contours j with ω_0 inside $\tilde{C}_j(\omega)$ is

$$\psi(x, t) = -\sum_j \int_{\tilde{C}_j(\omega)} \frac{d\omega}{2\pi} \frac{\exp[ik(\omega) x - i\omega t] \, S(k(\omega))}{\dfrac{\partial D^{\mathrm{SH}}(k(\omega), \omega)}{\partial k} (\omega - \omega_0)}$$

$$+ i \sum_j \int \frac{dk}{2\pi} \int_{C_j''(\omega)} \frac{d\omega}{2\pi} \frac{\exp[ikx - i\omega t] \, S(k)}{D^{\mathrm{SH}}(k, \omega)(\omega - \omega_0)}, \tag{A.17}$$

where $C_j''(\omega)$ is the dashed contour shown in Fig. 6b. It intersects the ω-points at P_1 and P_2 and lies inside the $\tilde{C}(\omega)$ contour but above $\omega = \omega_0$. In the first integral we have again transformed $k \to \omega$ through the relation $D^{\mathrm{SH}}(k, \omega) = 0$.

We lower $\tilde{C}_j(\omega)$ as before, but now we have the pole of $\omega = \omega_0$ to pick up as shown in Fig. 8b. The sign of the residue of this contribution is positive if $\tilde{C}_j(\omega)$ is clockwise and negative if the contour is counterclockwise. With further contour deformation we can write, for $\psi(x, t)$,

$$\psi(x, t) = i \sum_j \frac{\mathrm{sg}(\tilde{C}_j) \, S(k_j(\omega_0))}{\dfrac{\partial D^{\mathrm{SH}}(k_j(\omega_0), \omega_0)}{\partial k}} \exp[ik_j(\omega_0) x - i\omega_0 t]$$

$$+ \int_{\mathrm{real}\,k} \frac{dk}{2\pi} \frac{\exp[ikx - i\omega_0 t] \, S(k)}{D^{\mathrm{SH}}(k, \omega_0)} - \sum_j \int_{C_j'(\omega)} \frac{d\omega}{2\pi} \frac{\exp[ik(\omega) x - i\omega t] \, S(k(\omega))}{\dfrac{\partial D^{\mathrm{SH}}(k(\omega), \omega)}{\partial k}(\omega - \omega_0)}$$

$$+ i \int_{\mathrm{real}\,k} \frac{dk}{2\pi} \int_{\mathrm{real}\,\omega} \frac{d\omega}{2\pi} \frac{\exp[ikx - i\omega t] \, S(k)}{D^{\mathrm{SH}}(k, \omega)(\omega - \omega_0)}, \tag{A.18}$$

where the $C_j'(\omega)$ contour is shown in Fig. 8b. Again, the last term can be neglected as $t \to \infty$, and the next to last term is to be evaluated by the method of stationary phase. The second term is evaluated by deforming the path of integration, for $x > 0$ ($x < 0$) in the upper (lower) k plane (as in Fig. 7 for, say, $x > 0$). The exponentially growing terms in (A.18) then become as $t \to \infty$

$$\psi(x, t) \approx i \sum_j \frac{\mathrm{sg}(\tilde{C}_j) \, S(k_j(\omega_0))}{\dfrac{\partial D^{\mathrm{SH}}(k_j(\omega_0), \omega_0)}{\partial k}} \exp[ik_j(\omega_0) x - i\omega_0 t]$$

$$+ i \sum_{\substack{j \\ (x\,\mathrm{Im}\,k_j > 0)}} \frac{S(k_j(\omega_0)) \exp[ik_j(\omega_0) x - i\omega_0 t] \, \mathrm{sg}\, x}{\dfrac{\partial D^{\mathrm{SH}}(k_j(\omega_0), \omega_0)}{\partial k}}$$

$$+ \sum_j \frac{S(k_{\mathrm{b}j}) \exp[ik_{\mathrm{b}j} x - i\omega_{\mathrm{b}j} t]}{[i D_{kk}^{\mathrm{SH}}(k_{\mathrm{b}j}, \omega_{\mathrm{b}j}) \, D_\omega^{\mathrm{SH}}(k_{\mathrm{b}j}, \omega_{\mathrm{b}j}) \, t]^{1/2}(\omega_{\mathrm{b}j} - \omega_0)}. \tag{A.19}$$

Notice that certain members of the first term cancel the second term. Specifically, for, say, $x > 0$, the counterclockwise contours in the first term will have $\mathrm{Sg}\,\tilde{C}_j = -1$ and, from our previous discussion, it follows that $\mathrm{Im}\,k_j > 0$. These contributions will cancel with the second term, and only the contour contributions with $\mathrm{sg}(\tilde{C}_j) = +1$ persist in the first term. A similar cancellation occurs for $x < 0$. Now combining the result of Eqs. (A.16) and (A.19), the asymptotic time response as $t \to \infty$ is

$$
\psi(x, t) \approx i \sum_{\substack{[\omega_0 \text{ inside } \tilde{C}_j(\omega)] \\ x \,\mathrm{Im}\,k_0 < 0}} \frac{\mathrm{sg}\,x \exp[ik_j(\omega_0)\,x - i\omega_0 t]\,S(k_j(\omega_0))}{\dfrac{\partial D^{\mathrm{SH}}(k_j(\omega_0),\,\omega_0)}{\partial k}}
$$

$$
+ i \sum_{\substack{[\omega_0 \text{ outside } \tilde{C}_j(\omega)] \\ x \,\mathrm{Im}\,k_0 > 0}} \frac{\mathrm{sg}\,x \exp[ik_j(\omega_0)\,x - i\omega_0 t]\,S(k_j(\omega_0))}{\dfrac{\partial D^{\mathrm{SH}}(k_j(\omega_0),\,\omega_0)}{\partial k}}
$$

$$
+ \sum_j \frac{S(k_{\mathrm{b}j}) \exp[ik_{\mathrm{b}j} x - i\omega_{\mathrm{b}j} t]}{[iD_{kk}^{\mathrm{SH}}(k_{\mathrm{b}j},\,\omega_{\mathrm{b}j})\,D_{\omega}^{\mathrm{SH}}(k_{\mathrm{b}j},\,\omega_{\mathrm{b}j})\,t]^{1/2}(\omega_{\mathrm{b}j} - \omega_0)}. \tag{A.20}
$$

In Eq. (A.20) we observe amplification of waves in the direction of the predominant sign of the group velocity associated with the contour $\tilde{C}(\omega)$ if ω_0 is inside the $\tilde{C}(\omega)$ contour, and attenuation of those waves if ω_0 is outside of the contour.

Now, if we are given a frequency ω_0, with $\mathrm{Im}\,\omega_0 > 0$, we need to determine which of the k_{0j}, the zeros of $D(k_{0j}, \omega_0)$, are allowed as $|x| \to \infty$. The choice $x\,\mathrm{Im}\,k_{0j} < 0$ is the correct one if $(\omega_0, k_j(\omega_0))$ lies inside a contour $\tilde{C}_j(\omega)$ and the choice $x\,\mathrm{Im}\,k_{0j} > 0$ is the correct one if $(\omega_0, k_j(\omega_0))$ lies outside the contours $\tilde{C}_j(\omega)$. A point is inside (outside) a contour $\tilde{C}_j(\omega)$ if, as we vary ω from ω_0 to $\omega_0 + i\gamma$ with $0 < \gamma < \infty$, we follow $k_j(\omega_0 + i\gamma)$ and we cross the real k axis an odd (even) number of times. If $(\omega_0, k_j(\omega_0))$ is inside the contour, $x\,\mathrm{Re}\,v_{\mathrm{g}} > 0$ is guaranteed on the last crossing of the real k axis and there is a spatial wave amplification in the direction of the group velocity for $\omega = \omega_0$. From our discussion it is also clear that if $\mathrm{Im}\,\omega(k) \leqslant 0$ for all real k, and if $\mathrm{Im}\,\omega_0 > 0$, we are outside $\tilde{C}(\omega)$. Then only those k_j with $x\,\mathrm{Im}\,k_j > 0$ are correct; these are spatially attenuated waves.

We wish to establish a similar criterion on the wavenumber k for the response of a localized source in a periodic system with period L_0. The critical point is to show that the response function can be written in a manner similar to Eq. (A.6). The essential features are the poles at $\omega = \omega_0$ and $\omega = \omega(k)$, the continuum modes for real k.

To demonstrate such characteristics we first need to discuss some properties of $\hat{D}_{x,t}^{\mathrm{SP}}$. We define for any linear operator

$$
\hat{D}_x^{\mathrm{SP}}(\omega) = \lim_{T \to \infty} \frac{1}{T} \int_0^T dt \, \exp(i\omega t)\, \hat{D}_{x,t}^{\mathrm{SP}} \exp(-i\omega t). \tag{A.21}
$$

The eigenfunctions $\phi_{k,n}(x) \exp(ikx)$ with eigenvalue $\omega_n(k)$ satisfies the equation

$$\hat{D}_x^{SP}(\omega_n(k))[\phi_{k,n}(x) \exp(ikx)] = 0, \tag{A.22}$$

where k is real. We also observe that $\omega_n(k)$ can be analytically continued into the complex plane by choosing k complex and finding the complex ω-values that allow $\phi_{k,n}(x)$ to be periodic.

Now, let us consider the driven problem

$$\hat{D}_{x,t}^{SP}\tilde{\psi}(x, t) = \bar{S}(x) H(t) \exp i\omega_0 t. \tag{A.23}$$

By taking the time Laplace transform of this equation, we obtain

$$\hat{D}_x^{SP}(\omega) \psi(x, \omega) = i \frac{\tilde{S}(x)}{\omega - \omega_0}, \tag{A.24}$$

with

$$\psi(x, \omega) = \int_0^\infty dt \, e^{i\omega t} \tilde{\psi}(x, t). \tag{A.25}$$

We now write $\psi(x, \omega)$ as a Fourier integral,

$$\psi(x, \omega) = \int_{-\infty}^\infty \frac{dk}{2\pi} \psi_k(\omega) \exp(ikx), \tag{A.26}$$

and substitute this into Eq. (A.24). In general, from the periodicity conditions on $\hat{D}_x^{SP}(\omega)$ we have the property

$$\hat{D}_x^{SP}(\omega) e^{ikx} = \sum_m D_{k,mk_0}(\omega) e^{ikx + imk_0 x} \tag{A.27}$$

with $k_0 = 2\pi/L_0$. Thus, Eq. (A.24) can be written as

$$\int \frac{dk'}{2\pi} \sum_m D_{k',mk_0}(\omega) \exp[i(k' + mk_0) x] \psi_{k'} = i \frac{\tilde{S}(x)}{(\omega - \omega_0)}. \tag{A.28}$$

Now, multiplying Eq. (A.28) by $\exp(-ikx)$ and integrating in x yields

$$\sum_m D_{k - mk_0, mk_0}(\omega) \psi_{k - mk_0} = i \frac{S(k)}{(\omega - \omega_0)}, \tag{A.29}$$

where $S(k)$ is defined in Eq. (A.7).

Let us define the reduced wavenumber k_1 $(-\pi/L_0 < k_1 < \pi/L_0)$ and the matrix element $d_{n,m}(\omega)$ as

$$k_1 = \left(k + \frac{\pi}{L_0}\right) \bmod \left(\frac{2\pi}{L_0}\right) - \frac{\pi}{L_0}$$

$$d_{n,m}(\omega, k_1) = D_{mk_0 + k_1, (n - m)k_0}(\omega). \tag{A.30}$$

Equation (A.29) is then

$$\sum_m d_{n,m}(\omega, k_1) \psi_{k_1 + mk_0} = i \frac{S(k_1 + nk_0)}{(\omega - \omega_0)}, \tag{A.31}$$

where $n = (k - k_1)/k_0$. The inverse of $d_{n,m}(\omega, k_1)$ is

$$d_{n,m}^{-1}(\omega, k_1) = \frac{\tilde{d}_{n,m}(\omega, k_1)}{D^{SP}(\omega, k_1)}, \tag{A.32}$$

where $\tilde{d}_{n,m}(\omega, k_1)$ is the cofactor of $d_{n,m}$ and $D^{SP}(\omega, k_1)$ is the determinant of $d_{n,m}$. For $\omega = \omega_n(k_1)$, $D^{SP}(\omega_n(k_1), k_1) = 0$.

The solution to Eq. (A.31) can the be written as

$$\psi_{k_1 + nk_0}(\omega) = \frac{i}{D^{SP}(\omega, k)(\omega - \omega_0)} \sum_m \tilde{d}_{n,m}(\omega) S(k_1 + mk_0). \tag{A.33}$$

Thus, the solution to $\tilde{\psi}(x, t)$ is

$$\tilde{\psi}(x, t) = i \int_{\text{real } k \text{ axis}} \frac{dk}{2\pi} \int_{C(\omega)} \frac{d\omega}{2\pi} \frac{\sum_m \tilde{d}_{n,m}(\omega) S(k_1 + mk_0) \exp[ikx - i\omega t]}{D^{SP}(\omega, k_1)(\omega - \omega_0)}, \tag{A.34}$$

where $C(\omega)$ is a contour in the upper half ω-plane, as in Fig. 6, and recall $k = nk_0 + k_1$. Assuming these are no poles associated with the cofactor $\tilde{d}_{n,m}(\omega)$, the analyticity properties of Eq. (A.34) are identical to the analyticity properties of Eq. (A.6). Hence, our conclusions regarding the amplification or decay of the solution for large $|x|$ in the spatially periodic case are completely identical to those for the spatially homogeneous case.

REFERENCES

1. N. C. Christofolis, R. J. Briggs, R. E. Hester, E. J. Lauer, and P. B. Weiss, Lawrence Livermore National Laboratory Report UCRL-14282, 1965 (unpublished).
2. D. A. Phelps, A. C. Smith, Jr., D. M. Woodall, R. A. Meger, and H. H. Fleishmann, *Phys. Fluids* 17, 2226 (1974).
3. R. V. Sudan and J. M. Finn, *Nucl. Fusion* 22, 1443 (1982).
4. R. A. Dandl, H. O. Eason, P. H. Edmonds, and A. C. England, *Nucl. Fusion* 11, 411 (1971).
5. R. A. Dandl, H. O. Eason, P. H. Edmonds, A. C. England, G. E. Guest, C. C. Hedrick, J. T. Hogan, and J. C. Sprott, in *Proceedings, Plasma Physics and Controlled Fusion Research (IAEA, Vienna, 1971)*, Vol. I, p. 607.

6. M. Fujiwara *et al.*, in *Proceedings, Plasma Physics and Controlled Fusion Research (IAEA, Vienna, 1985)*, Vol. II, p. 551.

7. J. Kesner, *Nucl. Fusion* **20**, 557 (1980).

8. G. Benford, D. L. Book, N. C. Christofilis, T. K. Fowler, V. K. Neil, and L. D. Pearlstein, in *Proceedings, Plasma Physics and Controlled Fusion Research (IAEA, Vienna, 1969)*, p. 981.

9. D. B. Nelson and C. L. Hedrick, *Nucl. Fusion* **19**, 281 (1979).

10. M. N. Rosenbluth, S. T. Tsai, J. W. Van Dam, and M. G. Engquist, *Phys. Rev. Lett.* **51**, 1967 (1983).

11. K. V. Roberts and B. J. Taylor, *Phys. Fluids* **8**, 315 (1965).

12. A. H. Glasser, in *Proceedings, Finite Beta Theory Workshop (Varenna Summer School of Plasma Physics, September 1977, Varenna, Italy)* edited by B. Coppi and W. Sadowski (U.S. Dept. of Energy, Washington, DC, 1977), CONF. 7709167, p. 55.

13. Y. C. Lee and J. W. Van Dam, in *Proceedings, Finite Beta Theory Workschop (Varenna Summer School of Plasma Physics, September 1977, Varenna, Italy)* edited by B. Coppi and W. Sadowski (U.S. Dept. of Energy, Washington, D.C., 1977) p. 93.

14. J. W. Connor, A. J. Hastie, and J. B. Taylor, *Phys. Rev. Lett.* **40**, 396 (1978).

15. G. Rewoldt, W. M. Tang, and E. H. Frieman, *Phys. Fluids* **21**, 1513 (1978).

16. G. Rewoldt, W. M. Tang, and M. S. Chance, *Phys. Fluids* **25**, 480 (1982).

17. J. W. Connor, R. J. Hastie, T. J. Martin, and M. F. Turner, in *Heating in Toroidal Plasmas* (Commission of the European Communities, Brussels, 1982), Vol. I, p. 65.

18. G. Rewoldt and W. M. Tang, *Nucl. Fusion* **24**, 1573 (1984).

19. D. A. Spong, D. J. Sigmar, W. A. Cooper, D. E. Hastings, and K. T. Tsang, *Phys. Fluids* **28**, 2494 (1985).

20. J. Weiland and L. Chen, *Phys. Fluids* **28**, 1359 (1985).

21. D. P. Stotler, Ph.D. thesis, The University of Texas at Austin, 1986 (unpublished).

22. D. P. Stotler and H. L. Berk, *Phys. Fluids* **30**, 1429 (1987).

23. T. M. Antonsen and Y. C. Lee, *Phys. Fluids* **25**, 132 (1982).

24. P. J. Catto, R. J. Hastie, and J. W. Connor, *Plasma Phys. Controlled Fusion* **27**, 307 (1985).

25. B. Coppi, A. Ferreira, and J. J. Ramos, *Phys. Rev. Lett.* **44**, 990 (1980).

26. H. Grad, *Phys. Fluids* **10**, 137 (1967).

27. M. N. Rosenbluth, *Phys. Fluids* **11**, 869 (1968).

28. B. D. Fried and S. D. Conte, *The Plasma Dispersion Function* (Academic Press, New York, 1961).

29. E. L. Ince, *Ordinary Differential Equations* (Longmans, Green, 1927; reprinted, Dover, New York, 1944).

30. C. Z. Cheng, L. Chen, and M. S. Chance, *Ann. Phys. (N.Y.)* **161**, 21 (1984).

31. R. J. Hawryluk *et al.*, *Phys. Rev. Lett.* **49**, 326 (1982).

32. K. McGuire *et al.*, *Phys. Rev. Lett.* **50**, 891 (1983).

33. L. Chen, R. B. White, and M. N. Rosenbluth, *Phys. Rev. Lett.* **52**, 1122 (1984).

34. H. L. Berk, L. D. Pearlstein, J. D. Callen, C. W. Horton, and M. N. Rosenbluth, *Phys. Rev. Lett.* **22**, 877 (1969).

35. H. L. Berk and Y. Z. Zhang, *Phys. Fluids* **30**, 1123 (1987).

36. A. Bers, in *Handbook of Plasma Physics*, edited by M. N. Rosenbluth and R. Z. Sagdeev (North-Holland, New York, 1983), Chap. 3.2.)

37. D. Baldwin and G. Rowlands, *Phys. Fluids* **13**, 2036 (1970).

38. L. D. Landau, *J. Phys.* **10**, 25 (1946).

39. N. G. Van Kampen, *Physica,* **21**, 949 (1955).

40. K. M. Case, *Ann. Phys. (N.Y.)* **7**, 349 (1959).

41. H. L. Berk, L. D. Pearlstein, and J. G. Cordey, *Phys. Fluids* **15**, 1153 (1972).